ANALYTICAL AND DIAGNOSTIC STUDIES OF AN ICP-EXCITED ICP FLUORESCENCE SPECTROMETER

BY

ROBERT JOSEPH KRUPA

A DISSERTATION PRESENTED TO THE GRADUATE SCHOOL
OF THE UNIVERSITY OF FLORIDA IN
PARTIAL FULFILLMENT OF THE REQUIREMENTS
FOR THE DEGREE OF DOCTOR OF PHILOSOPHY

UNIVERSITY OF FLORIDA

1986

To my parents, whose loving support made all this possible.

ACKNOWLEDGEMENTS

I am grateful to Chester Eastman, Dailey Burch, and Vernon Cook of the Chemistry Department machine shop for their construction of much of the instrumentation used in this work.

I also wish to thank Dr. Benjamin Smith, Dr. Edward Voigtman, and Lori Davis whose stimulating discussions and comments have helped me enormously during my graduate career. Special thanks are extended to Dr. Nicolo Omenetto for his inspiring enthusiasm and many helpful suggestions concerning my research.

Steven Barber of R.F. Plasma Products deserves much of the credit for demounting the ICP load coils. His assistance in maintaining the ICP systems in our lab and in the initial set up of the present system is gratefully appreciated.

I owe a special debt of gratitude to Dr. James D. Winefordner whom I have had the privilege of working with during the past four years. His concern for his research group, his many innovative suggestions, and his encouragement during the course of this work have made my stay at the University of Florida a pleasurable and invaluable learning experience.

TABLE OF CONTENTS

LIST OF TABLES

LIST OF FIGURES

Abstract of Dissertation Presented to the Graduate School
of the University of Florida in Partial Fulfillment of the
Requirements for the Degree of Doctor of Philosophy

ANALYTICAL AND DIAGNOSTIC STUDIES OF AN
ICP-EXCITED ICP FLUORESCENCE SPECTROMETER

By

Robert Joseph Krupa

August 1986

Chairman: James D. Winefordner
Major Department: Chemistry

A 20 g/L solution of the element of interest is aspirated into a 1500 W inductively coupled plasma (ICP) and the resulting emission is used to excite atomic and ionic fluorescence in a second ICP which is used as the atomization cell. The fluorescence vs r.f. power curves exhibit three trends which describe the atomization efficiency of the elements investigated at different power levels. The non-refractory and refractory elements exhibit trends with a decrease and increase in fluorescence sensitivity vs power, respectively, while the alkaline earth elements' behavior is quite different, possibly because of a complex interaction of these elements with the decomposition products of water. Laser-excited atomic fluorescence (LEAFS) measurements of quantum efficiencies demonstrate that the ICP is an excellent atom and ion reservoir for fluorescence measurements with quantum efficiencies approaching unity. However, when propane is added to the plasma to increase the atomization efficiency of the refractory elements, the quantum efficiency is reduced and an increase in the atom/ion ratio is

observed. ICP-excited ICP atomic fluorescence spetrometry (ICP-ICP-AFS) detection limits are comparable to ICP-AES LODs; however, the combination of the fluorescence and resonance monochromator techniques yields linear dynamic ranges (LDRs) superior to atomic emission spectrometry (AES), approaching eight orders of magnitude in some cases. Spectral interferences are minimal with this system because of the selectivity of the fluorescence technique, making background correction unnecessary in most cases. Interelement effects are negligible in many cases because of the long sample residence time in the plasma; however, ionization interferences are slightly pronounced because of the relatively low temperature of the plasma at the observation height employed. The present system should be considered a viable alternative to conventional emission spectrometry when it is necessary to alleviate spectral interferences which may occur in complex sample matrices.

CHAPTER 1

INTRODUCTION

In the early 1960s, T.B. Reed developed the first inductively coupled plasma which employed argon tangentially flowing in a cylindrical torch [1]. The torch design was later modified and investigations into the analytical potential of the ICP were performed [2,3]. It was not until the 1970s that the ICP became a commercially available analytical instrument; since its introduction, ICP-AES has rivalled the detection limits of furnace AAS without the many matrix interferences encounted with electrothermal atomizers. Recently, the ICP has been established as an excellent line source for exciting fluorescence in flames [4-6] and a second ICP [7-9].

The efficient atomization and excitation properties of the ICP have yielded emission detection limits in the ng/mL range for most elements. The high intensity and stable emission from an analyte introduced into an emission ICP makes it more versatile than any other conventional source such as HCLs, EDLs, or Xe arc lamps. Several atomic line sources are lacking in intensity and stability, such as HCLs and EDLs for the non-metals, the lanthanides and actinides, and many refractory elements. In addition to the higher spectral irradiance of the ICP, the plasma is remarkably free of self-absorption at the observation heights commonly employed [4, 10]. This allows the aspiration of high concentrations, up to several percent, of the element of interest into the source ICP.

The ICP as an emission source for exciting fluorescence in a second plasma also has the advantage of emitting many ionic lines. This is an important consideration when the analyte element is highly ionized in the atomization cell. In fact, two-thirds of the strong transitions observed in the ICP are ionic transitions [11]. Low temperature sources of excitation, such as HCLs and EDLs, emit few ion lines and are predominantly atomic line sources; therefore, in many cases, these lamps do not permit the optimum fluorescence transitions to be probed. It is because of this limitation that the only commercially available atomic fluorescence instrument, manufactured by the Baird Corp., utilizes low r.f. powers and the addition of propane to the plasma [12]. At higher r.f. powers, the ionization of many elements is substantial, but the HCLs cannot efficiently excite these ionic species, and so low powers and low temperatures must be employed.

Because the emission of an element introduced into the ICP can be considered a narrow line source, many of the spectral interferences which commonly plague ICP-AES can be avoided. This spectral selectivity allows the analysis of even complex samples with the use of only a wide bandpass monochromator or interference filter, without the need for background correction.

By employing a second ICP as the atomization/ionization cell, a relatively high degree of freedom from matrix or interelement effects can be achieved. This is especially apparent when the ICP is compared to lower temperature cells such as flames, graphite furnaces, and microwave plasmas [13,14]. The higher temperature plasma is also a much more efficient atomizer, especially for the refractory metals which form very stable metal-oxide molecules.

Another unique advantage of employing two ICPs is the ability to determine trace species by the more sensitive fluorescence technique while analyzing the major sample constituents by the resonance monochromator technique [4-6]. When the fluorescence curve of growth becomes nonlinear because of self-absorption at high concentrations, the sample is used as the excitation source for exciting the fluorescence of a standard aspirated into the sample cell ICP. This combination of AFS and RM methods leads to linear dynamic ranges of up to eight orders of magnitude.

A description of the ICP-ICP-AFS instrument and an evaluation of the system's analytical figures of merit are now presented. Also, some diagnostic studies are presented which attempt to add to the existing knowledge we have of the ill-understood physical nature and excitation processes in the inductively coupled plasma.

CHAPTER 2

MATERIAL AND METHODS

A block diagram of the ICP-ICP-AFS instrument is presented in Figure 1. Both ICPs were operated at 27.12 MHz with automatic matching networks which tuned the capacitance of the generator to the plasma, reducing the reflected power. These units were both Plasma-Therm (Cherry Hill, N.J.) generators and matching networks, the source being a 2.5 kW unit (Model 2500K), with the atomization cell ICP being 1.5 kW (model T1.0).

In the past, translation of the ICP torch and load coil assembly was accomplished by moving the entire matching box/load coil assembly in the desired direction. This usually involved the use of cumbersome x-y milling tables and capstans which had poor spatial resolution and reproducibility. To facilitate the translation of the torches, the load coil assembly of each ICP was removed from the matching box. The load coil was mounted on a 6 x 6 x 0.5 in Teflon sheet. The plasma gases and cooling water were brought to the torch from the back side of the Teflon sheet through nylon bulkhead feedthroughs. The r.f. power was transmitted to the load coil from the matching box via two 12 x 0.75 x 0.01 in silverplated brass straps. The procedure described by Carr et al. [15] which employed tinned copper braid as the r.f. conductor proved unsuccessful. We were unable to ignite the plasma because of high reflected power which could not be tuned out with the capacitors in the matching

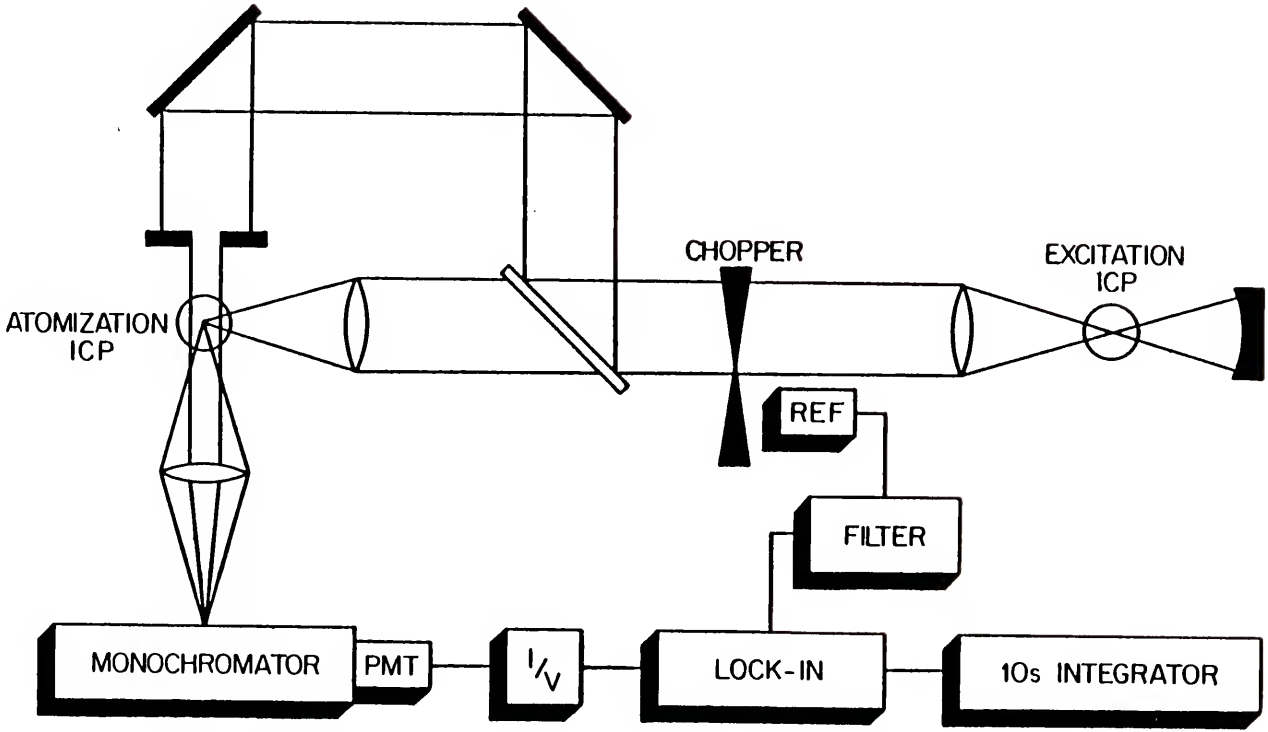

Figure 1. Block diagram of ICP-ICP-AFS.

network. This tuning mismatch may have been due to the added inductance introduced into the matching network by the copper braid. On a suggestion from Koirtyohann [16], who experienced similar tuning problems, we found brass straps to work without any increase in the reflected power. This system has been previously employed in several ICP spectrometers manufactured by the Baird Corporation (Bedford, MA) but did not reach the literature until recently [17]. With this system, the load coil assembly could be separated from the matching box up to a distance of 18 in without any matching problems. A conductor length of 12 in was chosen for this application which allowed vertical translation of the load coil up to 6 in and horizontal travel up to 4 in. To position the plasma, the Teflon mounting sheet was mounted on two micrometer-controlled translational stages (Newport Research Corporation, Fountain Valley, CA, model 440-2), connected at right angles to each other by an aluminum L-bracket. The two load coil assemblies, chopper, and optical components were mounted on a laboratory-constructed optical rail which was enclosed in a 28 x 13 x 23 in (length x width x height) aluminum box. The box served as a Faraday cage to contain the r.f. radiation which may add to the electronic noise in the detection electronics, and also reduced the stray light due to reflections of the source radiation which may increase the spectral background detected by the monochromator and photomultiplier tube. The interior of the box, which was painted flat black to reduce the reflectance of source radiation, was divided into two compartments by a grounded aluminum plate (with a window along the optical axis) placed between the two ICP load coils. This plate reduced the amount of scattered source radiation which may reach the monochromator and also served to reduce the coupling of the r.f. from

the two ICPs which produced a high frequency tone at the beat frequency of the two generators.

ICP-ICP-AFS System

The emission from a 20 g/L solution of the element of interest, which was aspirated into the source plasma operating at 1500 W, was used as the excitation line source for exciting the fluorescence. The source light was collected with a 2 in diameter, f 1, front-surface concave mirror and a 2 in diameter, f 1, fused silica lens. This collimated light was modulated at 168 Hz by a mechanical chopper (Princeton Applied Research, Princeton, NJ, model 125A) and focussed onto a second ICP, acting as the atomization cell for the sample solution, by a 2 in diameter, f 1.5, fused silica lens. An extended sleeve torch (Baird Corporation, Bedford, MA) was employed for the atomization cell in order to reduce the amount of air entrainment into the plasma and an observation height of 55 mm above the load coil was employed in order to increase the residence time of the sample in the plasma. The fluorescence radiation was collected at 90° by a single lens which formed a one-to-one image of the atomization cell plasma on the entrance slit of a low resolution (2.2 nm FWHM bandpass) monochromator (GCA-McPherson Corporation, Acton, MA, model EU-700). The light detected by the photomultiplier tube (Hamamatsu, Inc., Middlesex, NJ, model 928) was amplified by a current-to-voltage amplifier (PAR, model 181) and demodulated and filtered by a lock-in amplifier (PAR, model 186A) with an output time constant of 1 s. The lock-in output was displayed on a strip chart recorder (Fisher Scientific Co., Pittsburgh, PA, model 5000)

and filtered by a laboratory constructed 10 s integrator which was interfaced to a digital multimeter (Keithley Instruments, Inc., Cleveland, Ohio, model 175).

Absorption measurements employed the same detection system as in AFS; however, the collimated source radiation was folded by three front surface, plane mirrors before passing through the atomization cell ICP and into the monochromator (0.1 nm FWHM bandpass). The emission measurements from the atomization cell ICP were measured with the same collection optics as used for AFS and AAS; however, the lock-in amplifier was eliminated from the detection electronics.

Laser-Excited AFS System

A pulsed nitrogen laser (Laser Science, Inc., Cambridge, MA, model VSL-337) with a pulse width of 3 ns was employed to pump a dye laser (LSI, model DLM) and the emitted light, with a FWHM of 0.4 nm, was used to excite fluorescence in the extended sleeve torch atomization cell in order to determine the quantum efficiency of the ICP as a function of r.f. power and propane flow rate. In this study, the torch aerosol injection tube was positioned between the first and second turns of the load coil in order to produce the "pencil plasma" as employed by the Baird Plasma/AFS system (Baird Corp., Bedford, MA). The fluorescence was observed at an observation height of 80 mm above the top of the aerosol injection tube, or approximately 1 cm above the top of the torch. The previously described collection optics and monochromator were employed to obtain the fluorescence light which was detected by a photomultiplier tube (Hamamatsu, Inc., Middlesex, NJ, model 928) operated at -1000 V, its base modified for fast response [18] by adding

capacitors to the resistor network on the dynode chain. The photomultiplier tube output was connected to a 400 MHz storage oscilloscope (Tektronix, Inc., Beaverton, Oregon, model 7834) by a 1 m RG58U cable. The oscilloscope was triggered by a fast photodiode terminated into 50 ohms. The convolved laser pulse/photomultiplier tube response exhibited a 4 ns FWHM. The fluorescence lifetime measurement system was also used to determine the quantum efficiency of Na in the extended sleeve torch vs r.f. power with the aerosol injection tube positioned 5 mm below the load coil, as it is normally positioned.

Standard Operating Conditions

The operating conditions for the plasmas are listed in Table 1. These were the parameters employed for all measurements with the exception of the studies involving the effect of propane on the "pencil plasma." The pencil plasma employed the same extended sleeve torch as the atomization cell ICP as well as the same concentric Meinhard nebulizer. The cooling Ar was supplied at a rate of 10 L/min and there was no auxillary or plasma Ar used. The nebulizer was operated at 45 psig.

The source ICP nebulizer was fed with a peristaltic pump (Rainin Instrument Co., Boston, MA, model rabbit) which reduced the source flicker noise by approximately 10%. The major advantage of the pump, however, was to eliminate the salt encrustation of the aerosol injection tube. Previously the injection tube would clog after nebulizing the 20 g/L source solutions for 45 to 60 min, depending on the element. With the peristaltic pump, the nebulizer was operated at a lower sample uptake rate than pneumatic nebulization. This may have caused a

Table 1. ICP Operating Conditions.

	Excitation Source ICP	Atomization Cell ICP
Forward Power	1500 W	500 - 1500 W
Cooling Ar	10 L/min	10 L/min
Auxillary Ar	1.8 L/min	None
Observation Height (above the load coil)	17 mm	55 mm
Nebulizer	Cross-flow[a]	Concentric[b]
Nebulizer Pressure	11 psig	45 psig
Sample Uptake Rate	0.72 mL/min	1.35 mL/min

[a]Model TN-1, R.F. Plasma Products, Cherry Hill, NJ.

[b]Model T-230-A1, J.E. Meinhard Associates, Santa Ana, CA.

smaller aerosol droplet size which reduced the salt encrustation in the torch.

Sample and Standard Solutions

Stock solutions of 20 g/L (2%) were prepared by dissolving the pure metals or reagent grade salts in the minimum amount of acid and then diluting with deionized water. One exception to this procedure was the 20 g/L B solution which was prepared by dissolving boric acid in dilute ammonia because of this salt's limited solubility in water and dilute acids. Volumetric dilutions of these stock solutions were made in order to obtain the desired standard concentrations.

The National Bureau of Standards Standard Reference Material high carbon steel sample (SRM 364) was prepared by refluxing 3.0515 g of the sample for 10 h in 10 mL water and 20 mL concentrated, sub-boiling distilled nitric acid. After this time, the sample was transferred to a Teflon beaker and heated to dryness in the presence of 20 mL concentrated hydrofluoric acid. The dried sample was redissolved in 10 mL concentrated, sub-boiling distilled nitric acid and diluted to 250 mL with deionized water. A 10 mL aliquot of this solution was diluted to 100 mL with water and analyzed. The final sample concentration was 1.2206 g/L. A blank was also prepared using the same reagents and procedure. In all other cases, only a deionized water blank was employed.

CHAPTER 3

DIAGNOSTICS WITH THE EXTENDED SLEEVE TORCH

Influence of R.F. Power

The most important factor influencing the fluorescence signal in ICP-ICP-AFS was the r.f. power to the atomization cell ICP. Argon flow rates and observation height play an important role in the signal and background intensities, but to a much smaller degree [7-9,19]. It has become apparent, especially in ICP-AES, that there exists a strong dependence of the signal-to-background ratio on the operating parameters, leading several researchers to employ simplex optimization schemes [20-22] to determine the optimum combination of operating parameters for a particular analysis.

While optimizing the operating conditions for ICP-ICP-AFS, it became obvious that the elements investigated could be divided into three categories: refractory elements, non-refractory elements and the alkaline earth elements, depending on the shape of the fluorescence vs r.f. power plots. In order to investigate the cause of the behavior of the group II elements which were expected to follow the trends exhibited by the refractory or non-refractory elements, ICP-excited ICP-AFS, AAS, and ICP-AES were employed. The emission and fluorescence techniques have been well established as analytical and diagnostic methods; however, we believe this is the first reporting of the use of an ICP as

a source for atomic/ionic absorption employing a second ICP as an atom/ion reservoir, although there have been several attempts to use conventional sources with an ICP as an atom reservoir for AAS [23-25]. The advantage of using an ICP as an excitation source for AAS and AFS is that it is not limited to only atomic emission lines as are the low temperature hollow cathode lamps and electrodeless discharge lamps. This flexibility has allowed the study of not only atomic transitions but also ionic absorbance and fluorescence transitions as well.

For AAS, the relative source shot noise decreased with increasing source concentration aspirated into the source ICP because the signal-to-noise ratio (S/N) of I_o increases as the square root of the intensity ($S/N \propto \sqrt{I_o}$). However, collisional and self-absorption broadening increases the source linewidth as the source concentration is increased [26]. This leads to a decrease in the absorbance signal and a deterioration of the sensitivity. The source concentration which yielded the highest analyte absorbance S/N was typically 10 mg/L for the elements investigated. Absorbance curves of growth exhibited a linear relationship between absorbance and concentration from the detection limit up to approximately 500 mg/L. The detection limits for the alkaline earth elements and Cu (S/N=3) were between 1-10 mg/L. The relatively poor LODs are in part due to the short absorption pathlength through the absorption cell ICP, approximately 1 cm, and the flicker noise on the excitation source ICP.

The analyte solutions for AFS and AES were 1 mg/L, with the exception of P which was 10 mg/L. For AAS, 100 mg/L solutions were used because of the poor sensitivity. Curves of growth demonstrated that these concentrations were all within the linear dynamic ranges of the

three techniques. During this investigation, only one parameter, the r.f. power to the atomization cell ICP, was varied while all other operating parameters were held constant at the values listed in Table 1.

As a general rule, the elements which are easily atomized and which are determined in the air/acetylene or air/hydrogen flames are termed non-refractory. In contrast, those elements which form stable oxide molecules with dissociation energies (D_o) in excess of 6 eV and which require a nitrous oxide/acetylene flame for atomization are labelled refractory. The D_o values of several representative elements along with their ionization potentials are listed in Table 2, while Table 3 lists the wavelength of the transitions employed.

Most elements which were investigated by AFS fall neatly into these two categories. The non-refractory elements, exemplified in Figure 2 by Cu, Na, and Zn, show a decrease in fluorescence intensity with increasing r.f. power. The decrease is due to a decline in the ground state population because of an increase in the excited state and ionic populations at higher powers, thereby decreasing the ground state atom number density which can be probed by resonance fluorescence. The refractory elements, exemplified in Figure 3 by B, P, and Zr, show an increase in fluorescence intensity with increasing r.f. power because the refractory oxide molecules are more efficiently dissociated at higher powers, and hence, higher temperatures where there is more energy available to dissociate the strong metal oxide bond.

Figure 4, however, demonstrates the fluorescence behavior of the alkaline earth elements. This behavior was not typical of either the refractory or non-refractory trends, and appeared to be a combination of the behaviors portrayed in Figures 2 and 3. To determine whether this

Table 2. Ionization Potentials and Molecular Dissociation Energies.[a]

Element	I.P. (eV)	D_o(eV)		
		MO	MOH	$M(OH)_2$
B	8.298	8.1	--	--
Ba	5.212	5.8	4.9	9.7
Ca	6.113	4.8	4.3	9.4
Cu	7.726	4.9	--	--
Mg	7.646	3.9	2.4	--
Na	5.139	2.8	3.3	--
P	10.486	6.1	--	--
Sr	5.695	4.8	4.2	9.3
Zn	9.394	4	--	--
Zr	6.84	7.8	--	--

[a]Reference 27.

Table 3. Wavelength of Transitions Used in This Study.

Specie	Wavelength (nm)[a]
B(I)	Σ249.7-249.8
Ba(II)	455.4
Ca(I)	422.7
Ca(II)	393.4
CaO	455.0[b]
CaOH	555.0[b]
Cu(I)	324.7
Mg(I)	285.2
Mg(II)	Σ279.1-280.3
Na(I)	Σ589.0-589.6
P(I)	Σ253.4-255.5
Sr(II)	407.7
Zn(I)	213.9
Zr(II)	339.2

[a]The summation sign indicates that more than one transition falls within the monochromator spectral bandpass of 2.2 nm (AFS).

[b]Wavelengths from reference 28, all other from reference 29.

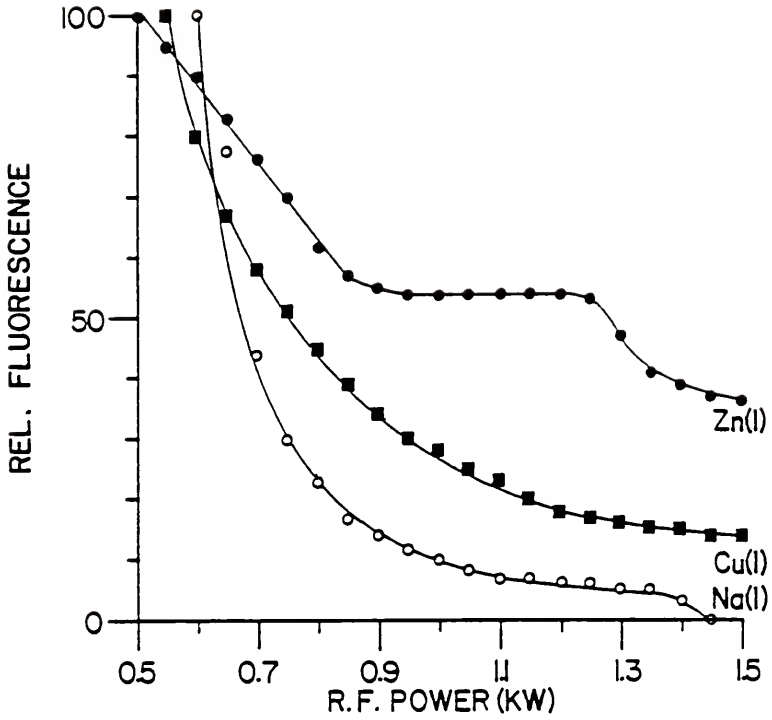

Figure 2. Non-refractory AFS vs power.

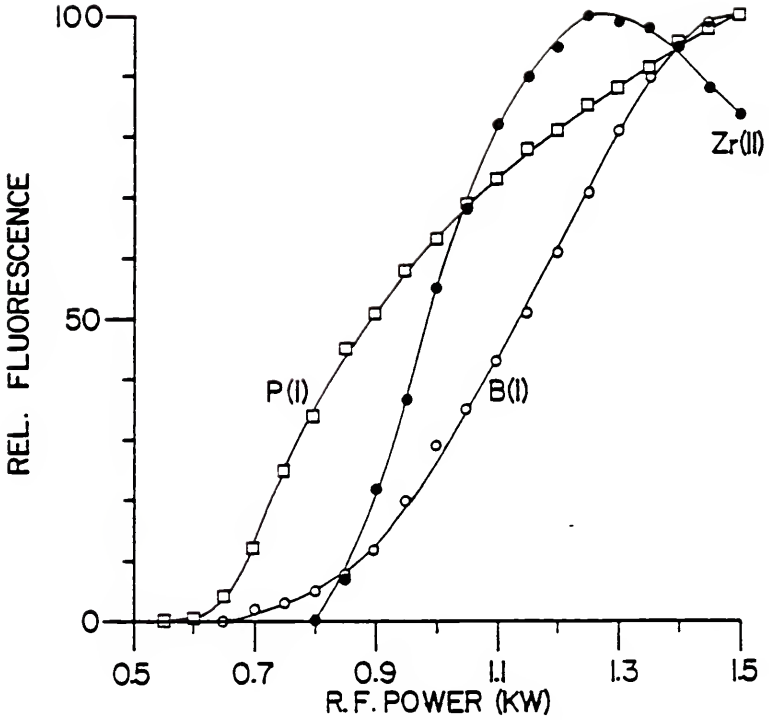

Figure 3. Refractory AFS vs power.

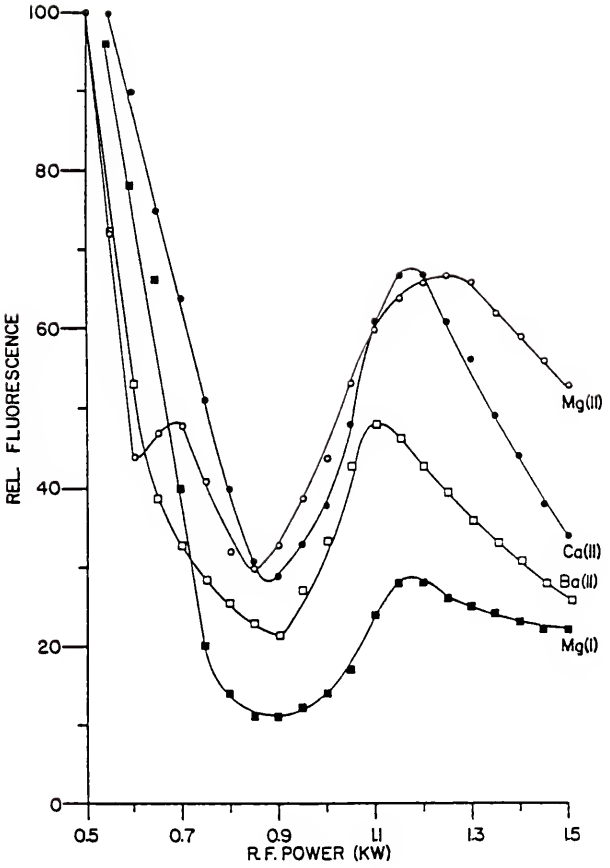

Figure 4. Alkaline earth AFS vs power.

behavior was due to a change in the physical nature of the plasma as the r.f. power was varied, such as abrupt changes in Ar metastable number density, quantum efficiency, etc., the Ar(m) absorbance was measured while varying the r.f. power and nebulizer conditions. Figure 5 shows the absorbance vs power for the conventional short torch and the extended sleeve torch used in this work. The Ar(m) absorbance (and therefore its population) increased smoothly with increasing power and was reduced when the nebulizer gas is turned on and when water is introduced into the plasma. However, the trends in the Ar(m) absorbances did not exhibit the dips or peaks in intensity which might account for the behavior of the alkaline earth elements. This was expected since the curves for the non-refractory and refractory elements follow the behavior expected according to their various dissociation energies and do not appear to be influenced by the changing nature of the plasma as the power is increased (other than the increase in plasma temperature).

Calcium was chosen as the test element for further investigation because of this element's high transition probabilities, relatively simple atomic and ionic spectra [29], and its well-studied behavior in both flames and plasmas [8,28,30-34].

Figures 6 and 7 show the behavior of Ca AAS and AFS intensities vs r.f. power. The fluorescence signals follow the absorbance signals quite closely indicating that these trends were due to the changing atom and ion populations in the plasma and were not due to selective quenching processes involving the excited state. If the quenching rate was changing as the r.f. power was increased, the fluorescence and absorbance curves would not exhibit the same trends because the

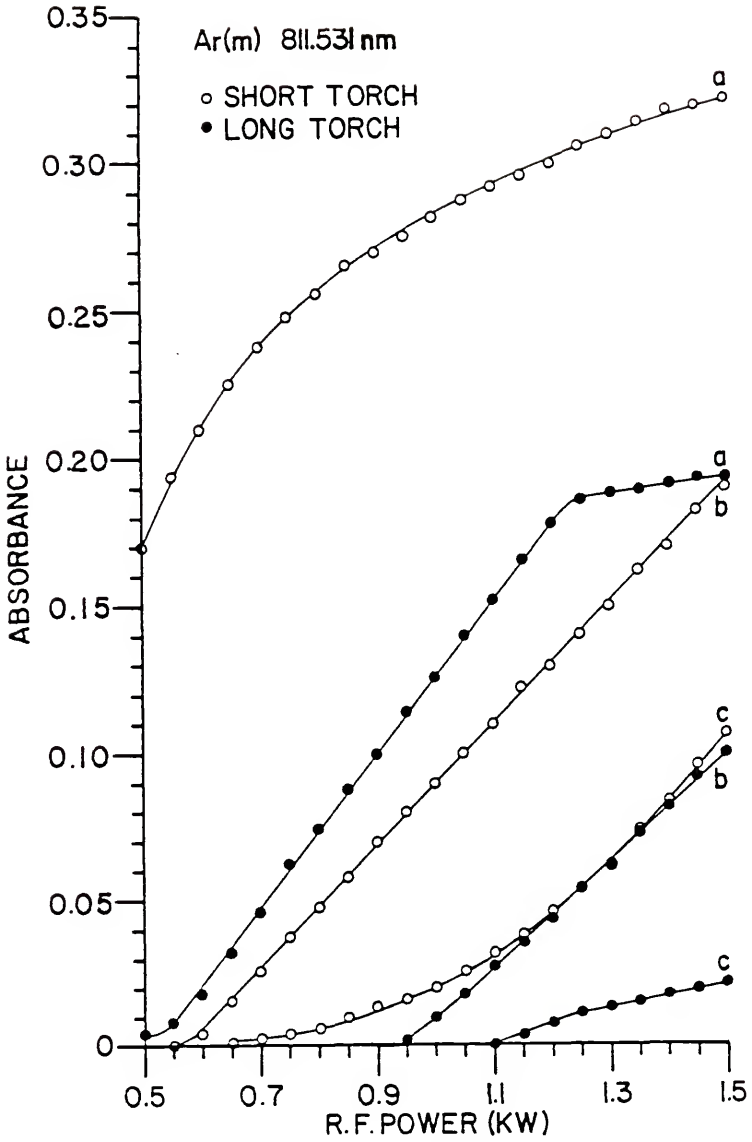

Figure 5. Ar(m) AAS vs power. a)no nebulizer Ar, b)nebulizer Ar flowing at 1 L/min, c)nebulizer Ar flowing at 1 L/min with water aspirated at 1 mL/min. Excitation ICP power at 800 W. Spectrometer bandpass is 0.1 nm.

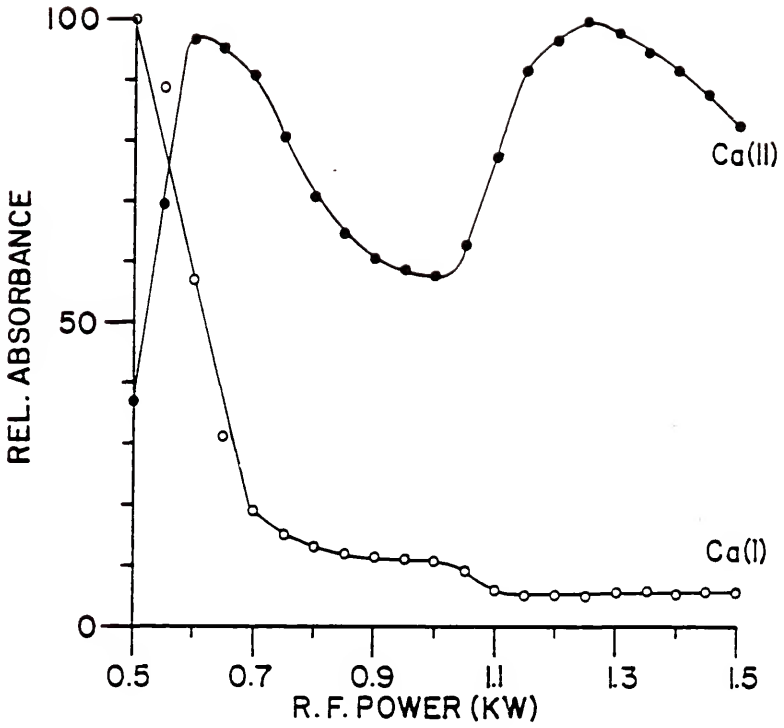

Figure 6. Ca AAS vs power.

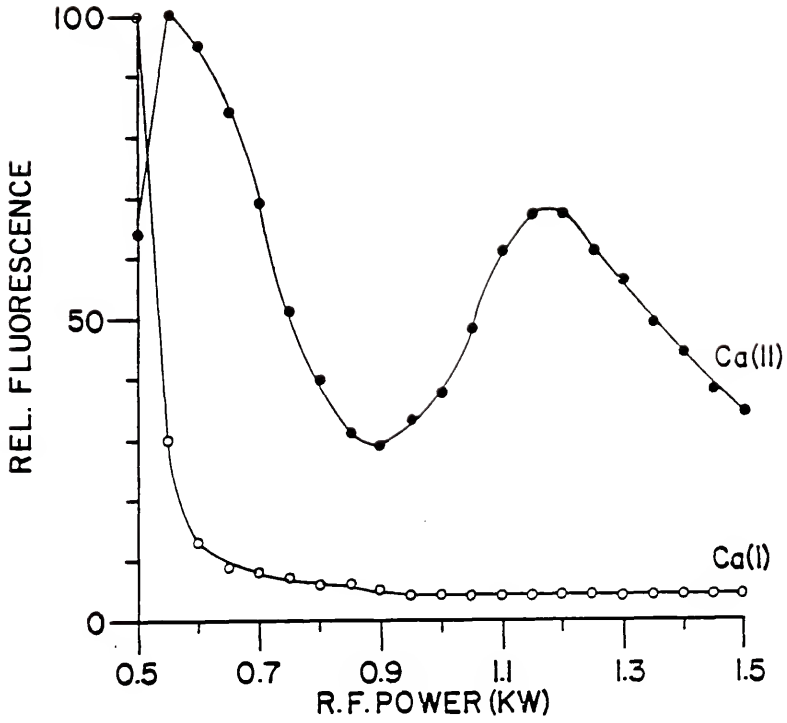

Figure 7. Ca AFS vs power.

quenching would only serve to decrease the fluorescence signal while leaving the absorbance signal unchanged. This is because absorption involves only the absorption of a photon, and this process does not involve the population of the excited state; it only depends upon the population of atoms or ions in the lower level from which absorption takes place. Fluorescence, on the other hand, is a two-step process which involves absorption as a first step; the second step, the emission or fluorescence of a photon, depends upon the quenching environment of the excited atom or ion. Further evidence that the quenching environment was not changing as the power was increased has been shown by Uchida et al. [35] who measured the lifetime of Na(I) vs r.f. power and found no change in the excited state lifetime. This was repeated using the present system by measuring the lifetimes of Na(I) and Li(I) using laser-excited fluorescence. It was demonstrated that the lifetimes of these two elements remained constant at 16 ns for Na and 24 ns for Li over a range of r.f. powers from 400 to 1500 W. Because the quantum efficiency is directly proportional to the observed lifetime, this indicates that the quantum efficiency of the atomization cell ICP does not change with changing r.f. power. A more detailed description of the quantum efficiency measurements is presented in Appendix B.

The emission signals vs r.f. power also showed a strong dependence on power as shown in Figures 8 and 9. The emission signals, however, were not necessarily correlated with the absorbance and fluorescence signals because the emission is related not only to the total population but also to the thermally excited population, whereas the absorbance and fluorescence signals are related to the ground state number density. The molecular species of Ca, as shown in Figure 8, exhibited the

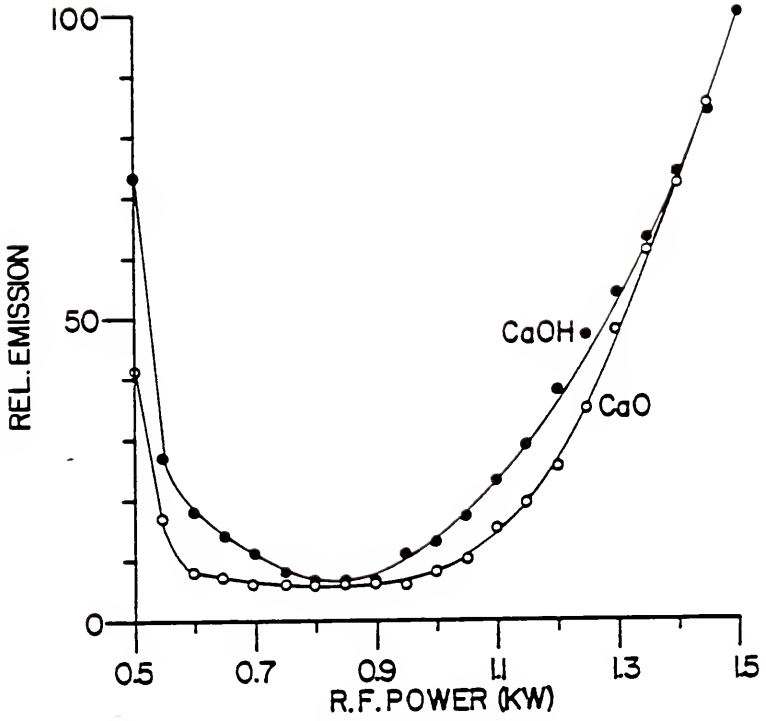

Figure 8. CaOH/CaO AES vs power.

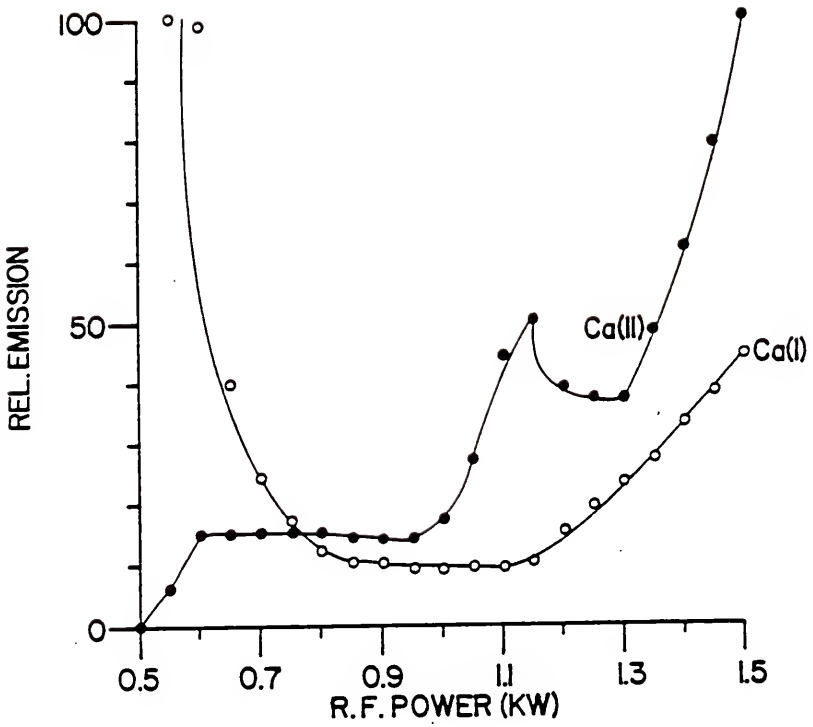

Figure 9. Ca AES vs power.

unexpected behavior of an increase in emission intensity at r.f. powers above 900 W. Although not strictly related to the ground state population, it was expected that the oxide and hydroxide populations in the plasma would decrease at the higher powers because of their relatively low D_o values. These emission plots seem to indicate that the Ca molecules become less abundant as the power increases from 500 to 900 W where the largest free atom population should occur. At higher powers, however, the increase in emission intensity may indicate a recombination of the free atoms/ions with the dissociation products of water. Similar trends have been observed for the absorption, emission, and fluorescence vs power plots of Mg(I), Mg(II), Sr(II), and Ba(II) using an ICP as an excitation source, and also with laser-excited AFS [36].

One possible explanation for this behavior is a complex "equilibrium" which may exist between the akaline earth atoms/molecules and the dissociation products of water. Although the plasma is not in local thermodynamic equilibrium, that is all radiative and nonradiative processes are not in equilibrium, certain equilibria still exist in the ICP. Examples of these equilibra, referred to as partial thermodynamic equilibria, which have been observed are Boltzman equilibrium of high-lying energy levels of Fe and between the ground state and metastable states of Ar [37].

At low r.f. powers, the sample aerosol is desolvated and the resulting molecular species were efficiently dissociated yielding a high atom or ion ground state population to be probed by fluorescence. As the power and temperature were increased, the decomposition of water into hydroxyl, oxygen, and hydrogen radicals may have increased which could have shifted the metal-metal oxide/hydroxide/dihydroxide

equilibrium toward the molecular species side, thereby decreasing the atom/ion population and the AFS signal. However, the higher temperatures also caused an increase in the excited state population relative to the ground state atom/ion and molecular populations. These processes at the higher powers may have resulted in the sudden increase in the fluorescence signals near 1200 W where the efficient molecular dissociation processes and the low hydroxyl and oxygen radical populations produced a high atom/ion population.

Quantum Efficiency of the ICP

As was discussed previously, lifetime measurements by LEAFS have demonstrated the high quantum efficiency of the Ar ICP when used as an atomization cell for fluorescence measurements (see Appendix B). This is because the inert Ar environment has a very low quenching cross-section as compared to combustion flames which contain large concentrations of very efficient quenchers such as N_2, CH, and C_2 [38]. However, it has been demonstrated by several researchers [8,12] that the addition of organic compounds enhanced the fluorescence signals of many elements. Typically, propane was added to the Ar carrier gas at a rate of 10-30 mL/min. For the refractory elements, the addition of propane appeared to scavenge the oxygen in the plasma forming either CO or CO_2. This reduced the free oxygen in the plasma which could react with the metal atoms which form stable refractory oxide molecules. However, even for several non-refractory elements, such as Li and Cu, which do not form stable oxide molecules in the ICP, there existed an enhancement in the fluorescence signals upon the addition of a small amount of propane to the plasma. The addition of organic molecules to the ICP was

expected to reduce the fluorescence signals of the non-refractory elements because of the decrease in quantum efficiency. In order to investigate the mechanism of this fluorescence enhancement, the quantum efficiency, electron number density, atom/ion populations, and OH signals were studied.

As was expected, the quantum efficiency (and the lifetime) of atoms the ICP was reduced when propane was added to the plasma as is demonstrated in Figure 10. A decrease in the excited-state lifetime of Li(I) with increasing propane flow was measured using LEAFS. In itself, this appeared to indicate that the fluorescence intensity should decrease as the propane flow increased, but just the opposite trend occurred. The reason for this increase in AFS signal seems to be linked to the increase in the electron number density (n_e) when propane was introduced. As is shown in Figure 11, the n_e increased with increasing propane flow which in turn reduced the population of Li(II) while increasing the Li(I) population. This is also demonstrated in Figures 12 and 13 which show the decrease in Ca (II) AFS signal while the Ca (I) signal increased with increasing propane. Because only the atom lines are observed in HCL-ICP-AFS, which is the technique which utilizes propane as a reductant, the increase in atom population offset the decrease in quantum efficiency, thereby producing a larger AFS signal for the non-refractory elements.

The reducing nature of the plasma when an organic gas is added produced an enhancement in the refractory elements' fluorescence as well. This was primarily due to the reduction of oxygen and hydroxyl radical concentrations in the plasma caused by the combustion of propane. When propane is added, the plasma emits the green light

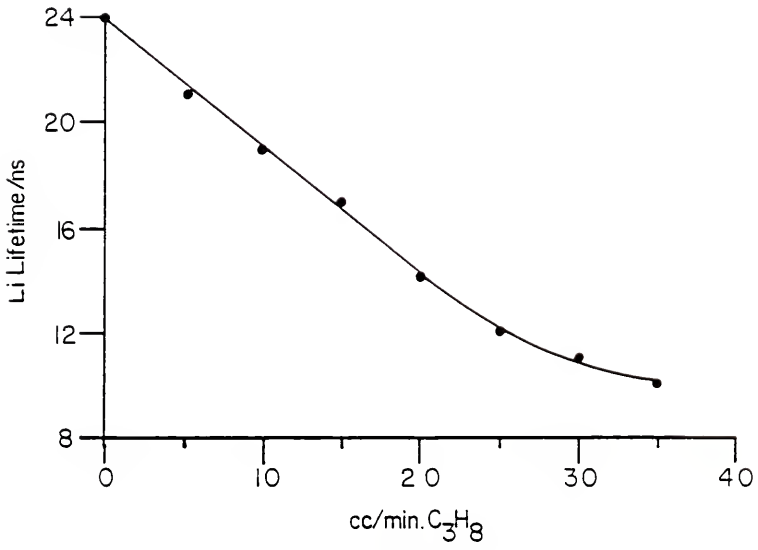

Figure 10. Li lifetime vs power.

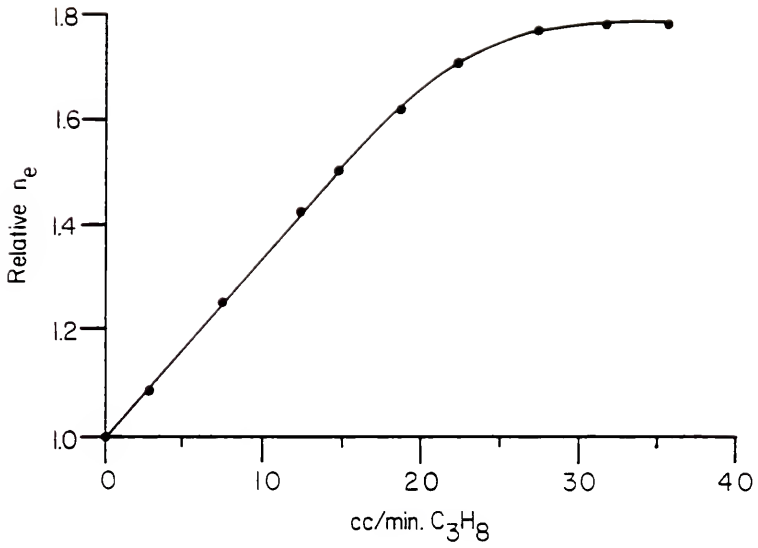

Figure 11. Electron number density vs propane flow. The relative number density was determined by the Starke broadening of the H(α) line.

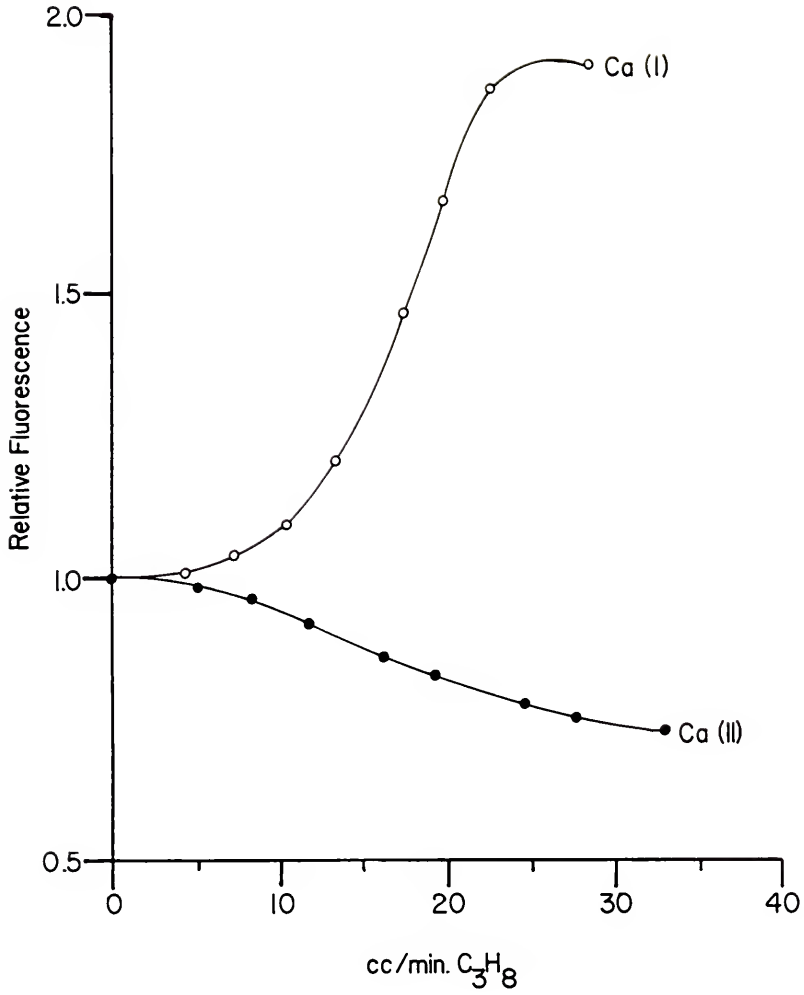

Figure 12. Ca AFS vs propane flow. Both the atomic and ionic fluorescence signals were normalized to a signal of unity at no propane flow.

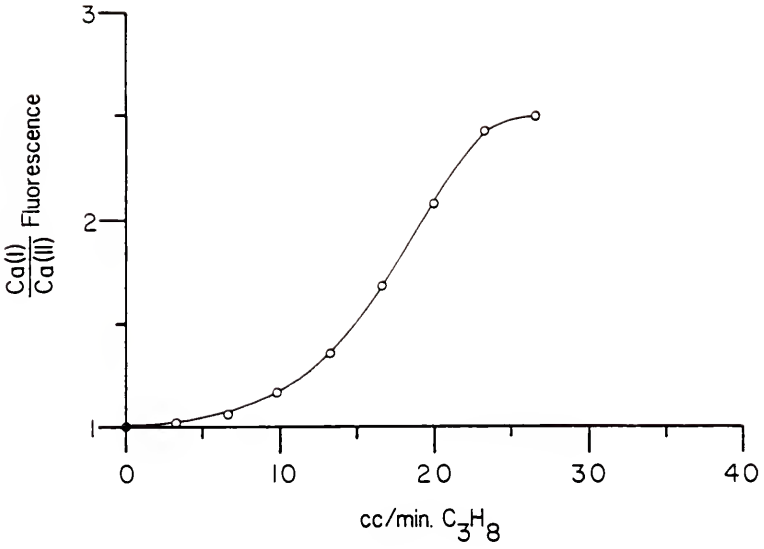

Figure 13. Ca atom/ion AFS vs propane flow.

characteristic of CH and C_2 emission. When the water to the nebulizer was stopped and only dry Ar was introduced into the plasma, this green emission increased dramatically, demonstrating qualitatively that there may have been a combustion process occurring between propane and water. This was quantitatively supported by the decrease in OH emission, as shown in Figure 14, as the propane flow increased.

Although the addition of propane to the ICP decreased the fluorescence quantum efficiency, the subsequent increase in electron number density increased the fluorescence signals for the non-refractory elements by suppressing ionization in the plasma. For the refractory elements, the propane decreased the amount of refractory oxide species by reacting with the oxygen and hydroxyl radicals, producing an increase in the free metal atom population which can be excited and produce fluorescence.

Conclusions

Although most of the elements investigated fall neatly into the categories of refractory or non-refractory depending upon their molecular dissociation energies and behavior with changing r.f. power, the alkaline earth elements' behavior appeared to be a combination of these two behaviors. This may have been due to a complex partial thermodynamic equilibrium between these atoms and the decomposition products of water. Although these results are inconclusive, they seem to indicate that water and its decomposition products play a major role in the atomization/excitation process in the extended sleeve torch ICP [39]. This is especially apparent for the Ar(m) population. Work is presently in progress to determine spatially resolved populations of hydroxyl,

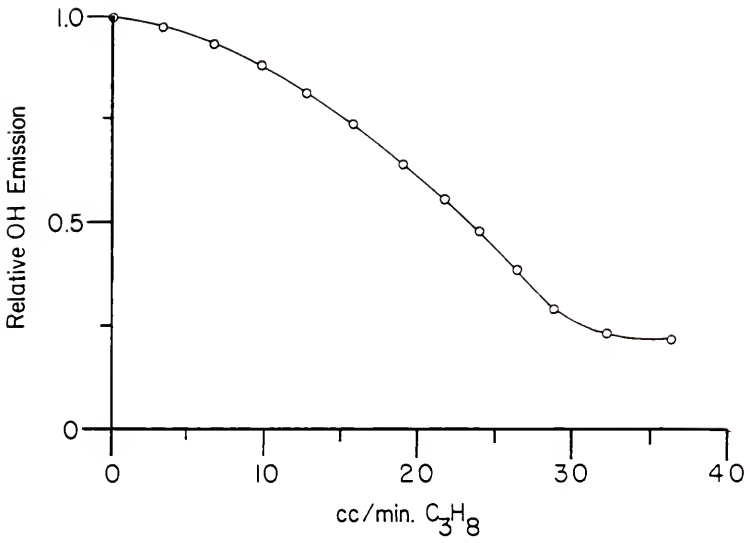

Figure 14. Hydroxyl AES vs propane flow. The OH emission was observed at 306.3 nm while aspirating water into the ICP.

hydrogen, and oxygen species in the ICP. These measurements may provide an explanation of these unexpected curves, and contribute to a better understanding of the extended sleeve torch atom reservoir.

By measuring the lifetime of Na and Li, it was demonstrated that the low quenching cross-section Ar ICP is an excellent atom/ion reservoir for fluorescence measurements, the quantum efficiency for Na(I) between 400-1500 W being unity. Even when the quantum efficiency was lowered by introducing propane into the plasma, the ICP retained its integrity as an atomization cell. This was because the increase in n_e and the reduction of oxygen in the plasma increased the atom/ion ratio and diminished the formation of refractory oxide species. This is especially important to atomic fluorescence measurements with hollow cathode lamp excitation; however, with a second ICP as the excitation source, ionic transitions can be used and the reduction of refractory molecules can be accomplished by increasing the r.f. power.

CHAPTER 4

FIGURES OF MERIT FOR ICP-ICP-AFS

Detection Limits for ICP-ICP-AFS

As was demonstrated in Figures 2 and 3, the non-refractory elements exhibit their maximum fluorescence signal at low r.f. powers while the more difficult to atomize refractory elements exhibit their maximum sensitivity at approximately 1200 W. For this reason, the LODs of the non-refractory elements were determined at 700 W while those of the refractory elements were measured at 1200 W. The detection limits are defined as the concentration which gives a signal equal to twice the standard deviation of sixteen consecutive blank readings. The LODs obtained by ICP-ICP-AFS for twenty-two elements are listed in Table 4 along with those obtained by HCL-ICP-AFS and ICP-AES. A comparison of detection limits for several spectometric methods is presented in more detail in Appendix C.

With the exception of Na and K, the detection limits for the non-refractory elements are similar for all three methods. For Na, the fluorescence techniques were superior to emission because of the high degree of ionization of this element low in the AES plasma. By using an observation height higher in the plasma tail, the temperature and degree of ionization decreased [40], yielding a larger atom population to be probed by AFS. Potassium also suffered from a high degree of ionization which resulted in a poor AES LOD. In ICP-ICP-AFS, the high degree of

Table 4. Comparative Detection Limits in ng/mL (S/N=2).

Element	λ_{AFS}, nm[a]	ICP-ICP-AFS	HCL-ICP-AFS[b]	ICP-AES[c]
		Non-refractory elements		
Ca	393.4	0.4	0.4	0.1
Cr	357.9	10	5	4
Cu	324.7	0.4	1	4
K	766.5	100	0.8	300[d]
Mg	Σ279.1-280.3	0.2	0.3	0.1
Na	Σ589.0-589.6	1	0.3	20
Pt	214.4	30	75[e]	20
Sr	407.7	0.2	2	0.3
Zn	213.9	2	0.4	1
		Refractory elements		
Al	Σ394.4-396.2	10	15	20
B	Σ249.7-249.8	10	2000	3
Ba	455.4	0.9	50	0.9
Hf	Σ263.9-264.1	30	--	10
Ho	Σ345.3-345.6	10	--	4
P	Σ253.4-255.5	80	--	50
Si	Σ251.4-252.9	7	300	8
Sm	Σ359.3-360.9	20	--	30
Th	Σ283.2-284.3	100	--	40
V	Σ309.3-310.2	40	300	3
Y	Σ360.1-361.1	20	500	2
Yb	369.4	10	--	1
Zr	339.2	10	--	5

[a]This work only. The summation sign indicates that more than one fluorescence transition falls within the monochromator spectral bandpass.

[b]Reference 41.

[c]Reference 11.

[d]Reference 42.

[e]Reference 43.

ionization in the source ICP resulted in a poor atomic source irradiance as compared to the HCL emission. Even when 1% Cs was added to the 2% K excitation solution, there was no increase in the fluorescence sensitivity.

The LODs for the refractory elements for ICP-ICP-AFS and ICP-AES were quite similar, with the exception of V. The most intense V fluorescence signal was at the 309-310 nm lines which were in the midst of the OH band. The increased plasma emission in this region increased the background shot noise and produced a higher LOD.

The HCL-ICP-AFS LODs for the refractory elements differ significantly from the other two methods. This is primarily due to the poor atomization efficiency of these elements and the use of HCLs as excitation sources. At low r.f. powers, the refractory oxide molecules are not efficiently dissociated, while at higher powers, there is a significant degree of ionization for many of these elements. The HCL's output, however, is primarily atomic resonance radiation and these ionic transitions cannot be probed. For elements such as aluminum, this is not a significant drawback because of this element's high ionization potential. For elements like Ba and Sr, the HCL's inability to excite efficiently these ionic transitions results in comparatively higher LODs because the atomic transitions must be used. In general, HCL-excited ICP-AFS will be comparable to ICP-AES and ICP-ICP-AFS when the elements of interest form molecular oxides with low dissociation energies compared to their ionization potentials. Another major drawback of HCL-ICP-AFS is the lack of availability of high irradiance HCLs for many elements. This is a contributing factor in the poor detection limits

obtained by HCL-ICP-AFS for B and Si, and the cause for the lack of information for many elements such as the lanthanides.

ICP-ICP-Resonance Monochromator

In many applications, there is a need to determine both trace elements as well as the major sample constituents. Even with the large LDR of AES and AFS, it is often necessary to prepare several sample dilutions or to use less sensitive analytical lines in order to accomplish this. Sample dilution is time consuming and may introduce dilution errors and contaminate the sample, while choosing less sensitive emission or fluorescence lines may increase the influence of matrix effects and spectral interferences because of the lower signal-to-noise ratio. An alternative is to employ the resonance monochromator (RM) technique to increase the LDR. Figure 15 illustrates typical curves of growth for Ca AFS and RM. When the AFS curve begins to bend toward the concentration axis because of self-absorption [44], the sample solution can be aspirated into the source ICP and its emission used to excite the fluorescence of a 100 mg/L standard solution which is aspirated into the atomization cell ICP. By doing this, the LDR can be extended by one to two orders of magnitude. Typical detection limits are listed in Table 5, along with comparative upper linear concentrations.

Because the emission from the excitation ICP has a similar spectral bandwidth as the absorbing atoms in the atomization cell ICP, the entire spectral line is integrated [44], which leads to upper linear concentrations as high as 10,000 mg/L. Atomic emission spectrometers generally employ a very narrow spectral bandpass in order to reduce spectral interferences. As the concentration of the analyte increases and the

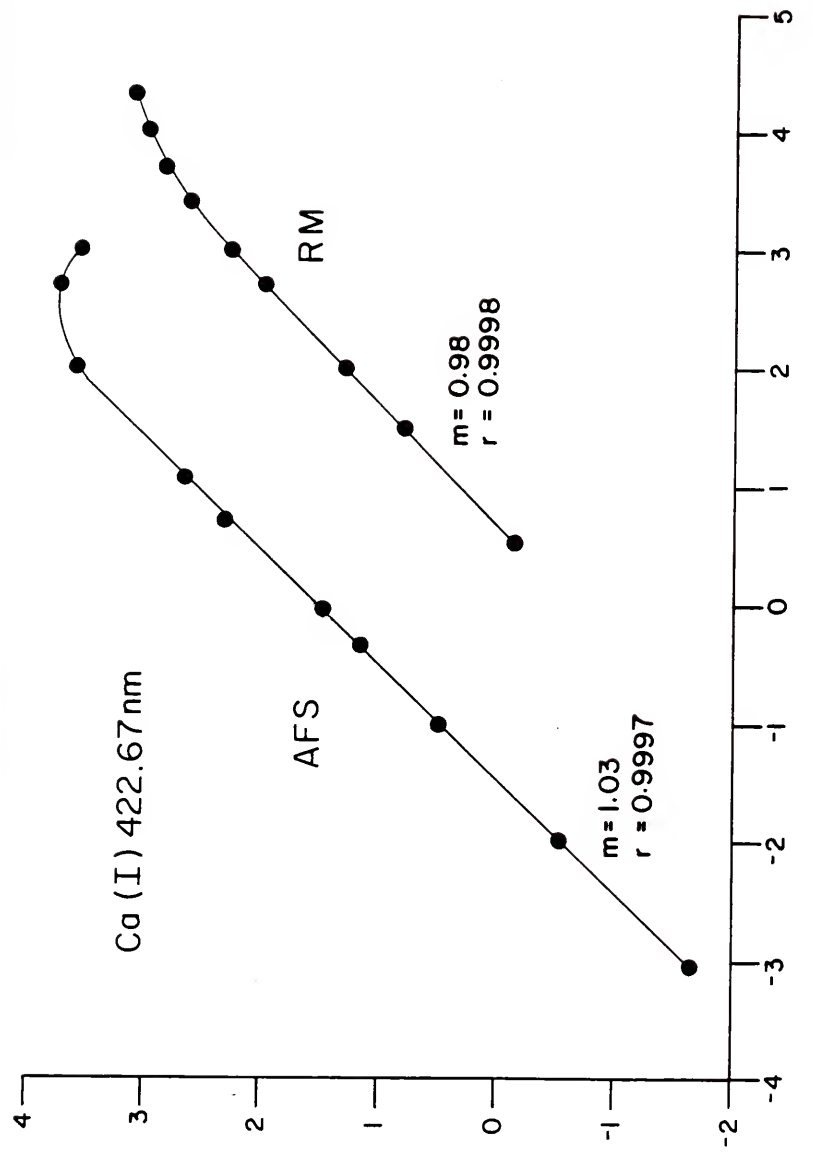

Figure 15. Ca AFS and RM curves of growth.

Table 5. Resonance Monochromator Detection Limits (mg/L) and Comparative Upper Linear Concentrations (mg/L).

Element	ICP-ICP-RM LOD	Upper Linear Concentration ICP-ICP-RM	HCL-ICP-AFS[a]	ICP-AES[b]
Ba	1	5,000	--	100
Ca	1	3,000	90	20
Cr	2	5,000	500	150
Cu	3	5,000	75	150
Mg	3	10,000	20	50
Na	20	2,000	10	200
Zn	4	5,000	20	150

[a]Reference 45.

[b]Reference 43.

spectral line begins to broaden, the emission spectrometer only views the line center. When self-absorption begins to occur, it affects the line center while the wings of the broadened line continue to increase in intensity, but this is not seen by the detector. A similar spectral bandpass limits the LDR of HCL-ICP-AFS; however, in this instance, the narrow source profiles of the HCLs are the limiting factor. The HCLs, because they are at low pressure and at a significantly lower translational temperature than the atoms in the ICP, have a much narrower emission profile than the absorption profile of the atoms in the ICP. Therefore, even though a wide spectrometer (filter) bandpass can be employed without increasing the effect of spectral interferences, only the line center is being measured as in AES. Another limiting factor is the use of large bandpass filters in HCL-ICP-AFS which can have a bandpass of 2-12 nm. This tends to pass a large fraction of the plasma background and analyte emission signal which can saturate the photomultiplier tube at high analyte concentrations, even though the AFS signal may still be linear.

Spectral Interferences

Elaborate background correction techniques are often necessary in ICP-AES in order to reduce the effect of spectral interferences. This usually requires a computer-assisted scan of the spectral region near the line of interest and a deconvolution of the interfering and analyte emission lines. Fluorescence spectra, when a line source of excitation is used, are inherently simple, containing only the fluorescence lines of interest in most cases. Comparisons of ICP-AES and ICP-ICP-AFS backgrounds are shown in Figures 16 and 17. In scan (a) of Figure 16,

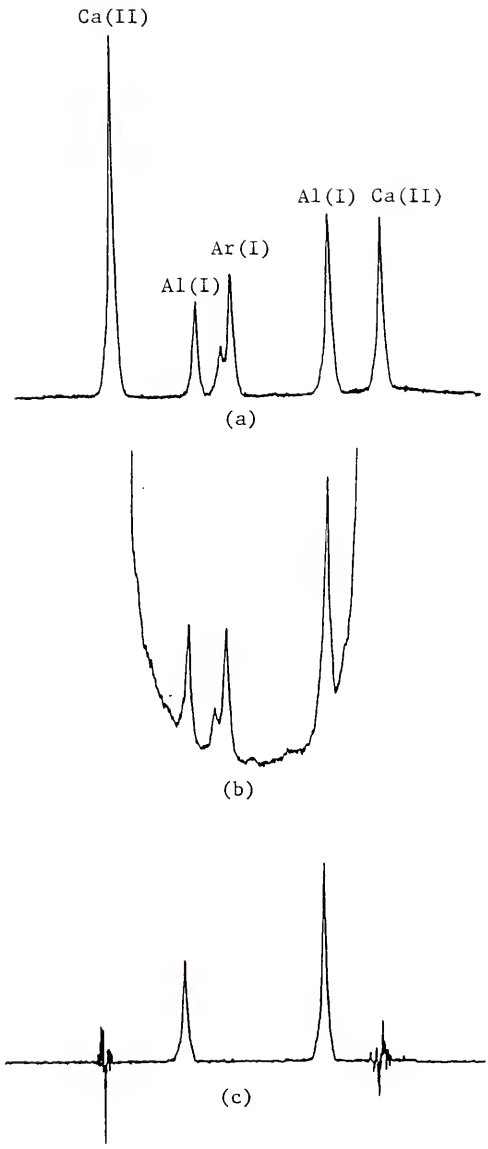

Figure 16. Ca spectral interference on Al. a) 1 mg/L Ca and 50 mg/L Al AES, b) 1000 mg/L Ca and 50 mg/L Al AES, c) 1000 mg/L and 50 mg/L Al AFS with 2% Al excitation.

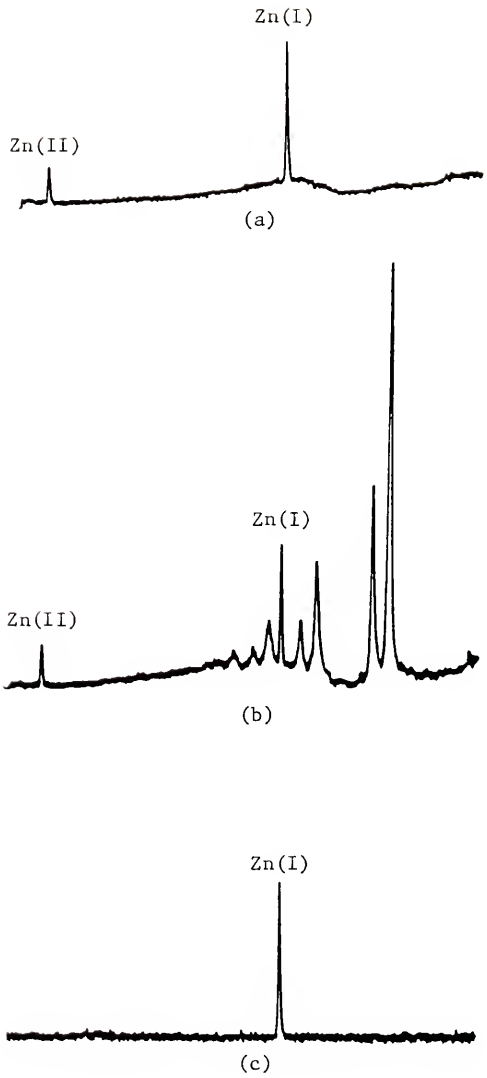

Figure 17. Al spectral interference on Zn. a) AES from 10 mg/L Zn, b) AES from 10 mg/L Zn and 1000 mg/L Al, c) AFS from 10 mg/L Zn and 1000 mg/L Al with 2% Zn excitation.

the emission spectrum of a solution containing a low concentration of Ca and Al exhibits the doublets of these two elements as well as an Ar doublet. Scan (b) shows the effect of increasing the Ca concentration on the Al peaks. The Al doublet now lies in the valley between the two collisionally broadened Ca peaks [46] making background correction a necessity. The fluorescence spectrum (c) of the same solution, using 2% Al in the excitation source ICP, demonstrates that there was no increase in the background around the Al peaks, although the background shot noise at the Ca wavelengths was increased. Also absent in the AFS spectrum were the Ar emission doublet and the plasma recombination continuum.

This type of spectral interference is well documented in the literature [11,46,47] and can be corrected by appropriate background correction techniques developed for AES. Many spectral interferences, however, are not listed in the prominent line tables and must be evaluated on a sample by sample basis. This is illustrated in Figure 17 by the Al interference on Zn AES. Scan (a) shows the emission spectrum of 10 mg/L Zn demonstrating the relative simplicity of the plasma background near 200 nm. However, when 1000 mg/L of Al was added to this Zn solution, the background recombination continuum increased and several Al transitions appeared around the Zn(I) line. The wavelength separation of the Al and Zn peaks is sufficiently large that no direct spectral overlap occurs, but the increase in background must be subtracted from the Zn AES signal. Although no spectral interference occurred, this points out the potential for interferences to occur from interfering lines which are not considered "prominent lines" and are not commonly tabulated in the literature. The AFS spectrum of the Zn and Al

solution, shown in scan (c), once again demonstrates the simplicity of fluorescence spectra which enables one to use AFS to analyze real samples without the need for background correction in most cases.

There are several types of background sources in the ICP which may cause spectral interferences in AFS. The plasma and other ion recombination continua [46] are emission phenomena and do not produce fluorescence signals. Molecular fluorescence of species such as metal oxides or OH radicals are not efficiently excited by the source ICP to produce any noticeable fluorescence signal. For example, no fluorescence signal was observed for AlO, even at an Al concentration of 10 g/L. Atomic or ionic emission lines within the spectrometer bandpass only add to the background shot noise and do not add to the modulated fluorescence signal. Their presence can be reduced by increasing the integration time on the electronic measurement system, but their presence will degrade detection limits depending upon the interferent concentration in the matrix by increasing the blank noise. Direct spectral overlap of two elements does present a small problem in ICP-ICP-AFS. Several contrived cases of direct spectral overlap are presented in Table 6. The majority of the interferent wavelengths do not appear in Boumans' "Line Coincidence Tables" [47] or in the "Prominent Lines Table" of Winge et al. [11]. Many of the reported spectral interferences encountered in ICP-AES [47] were evaluated using ICP-ICP-AFS, but only a small fraction of these interferences were detectable at concentrations below 10 g/L.

For a spectral interference to occur in AES, the interfering transition must fall within the spectral bandpass of the monochromator. In AFS, the criteria for spectral interferences are much more stringent and depend upon a) the interfering specie's absorption cross section

Table 6. Spectral Interferences in ICP-ICP-AFS.

Source Element	Source Wavelength (nm)[a]	Interferent	Interferent Wavelength (nm)[a]	Wavelength Separation (nm)	Interferent LOD (mg/L)[b]
Al	396.1527	Mo	396.1503	0.0024	2,000
		Zr	396.1587	0.0060	>10,000
Ba	455.4042	Mo	455.4028	0.0014	>10,000
		Zr	455.3967	0.0075	8
		Cr	455.3949	0.0093	>10,000
Ca	393.3666	Hf	393.3664	0.0002	3
		Co	393.3654	0.0012	9
		Fe	393.3605	0.0061	20
Ca	422.6728	Cr	422.6758	0.0030	>10,000
		Al	422.6809	0.0081	60
Cu	324.7540	Mn	324.7542	0.0002	>10,000
Mg	279.0787	Fe	279.0930	0.0143	
		Fe	279.1008	0.0221	>10,000
	279.5530	Fe	279.5544	0.0014	
	279.8060	Mo	279.8110	0.0050	
		Mo	279.7913	0.0147	>10,000
	280.2695	Cu	280.2683	0.0012	800
Si	250.6889	V[c]	250.6905	0.0016	
	251.4331	V	251.4318	0.0013	
	251.6123	V	251.6118	0.0005	
	252.8516	V	252.8468	0.0048	
		V	252.8836	0.0320	600
Y	360.1921	Sm	360.1984	0.0063	
	361.1047	Sm	361.1056	0.0009	>10,000

Continued

Table 6. Continued.

Source Element	Source Wavelength (nm)[a]	Interferent	Interferent Wavelength (nm)[a]	Wavelength Separation (nm)	Interferent LOD (mg/L)[b]
Zn	213.8560	Cu	213.8507	0.0053	100
		Ni	213.8580	0.0020	3,000
		Fe	213.8589	0.0029	>10,000

[a]Reference 48.

[b]That interferent concentration which gave a signal equal to two times the standard deviation of the blank when excited by a 2% solution of the source element.

[c]There are a total of 27 V lines within the monochromator bandpass.

over the emission source's spectral profile; b) the population of the interfering species in the proper energy level; and c) the fluorescence quantum efficiency of the interfering species within the detector's spectral bandpass. Therefore, substantially fewer spectral interferences occur in AFS as compared to AES.

Interelement Effects

The inert, high temperature environment of the ICP makes it an excellent atomization cell for atomic spectrometry. A relatively high degree of freedom from interelement (matrix) effects is a major advantage of the ICP over flame, furnace, and microwave discharge atom reservoirs [13,14].

The solute vaporization interferences of sulfate and phosphate [14] on Ca were investigated by measuring the fluorescence signal at 393.4 nm of a 1 mg/L Ca solution while varying the interferent concentration. Solutions containing up to 50,000 mg/L SO_4^{-2} or PO_4^{-3} produced no depression or enhancement of the fluorescence signal. This is due to the high temperature of the plasma and the long residence time of the sample in the plasma plume.

Figure 18 illustrates the interference of Na on Ca which resulted from the shifting of the ion/atom equilibrium [49]. There was a minimal effect upon the Ca fluorescence signal at Na concentrations below 10 mg/L. However, at higher concentrations, the effects became pronounced. The onset of the Na interference occurs at a Na number density of approximately 1×10^{12} cm^{-3}, which is comparable to the n_e trends reported in reference 49 at a temperature of 4000 K (Fe Boltzman plot).

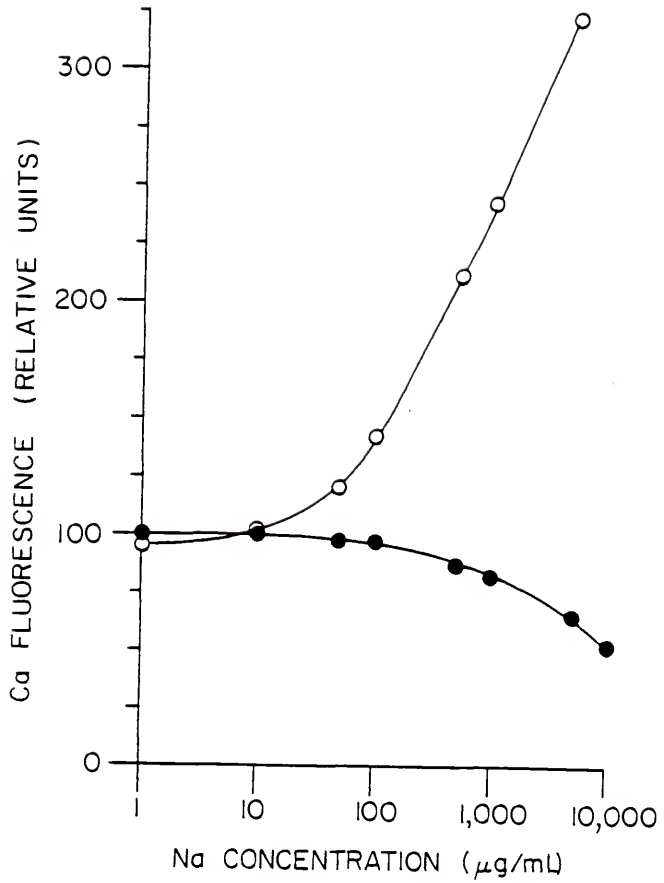

Figure 18. Effect of Na on Ca AFS. O Ca(I), ● Ca(II).

The ionization interference occurs because of the introduction of an element which is easily ionized in the plasma, and which produces a shift in the ion/atom equilibrium. This equilibrium is described by the Saha equation, which states that the ratio of ions to atoms in a given system is constant at a specified temperature and n_e:

$$\log \frac{n_+ n_e}{n_o} = \frac{-5040IP}{T} + \frac{5}{2} \log T + \log \frac{Q_+}{Q_o} - 6.1818$$

where n_+ and n_o are the number densities of the ions and atoms, respectively, IP is the ionization potential of the atom (in eV), T is the temperature (in K), and Q_+ and Q_o are the ionic and atomic partition functions, respectively. When Na is introduced into the plasma, n_e increases due to the ionization of Na atoms, which have a low I.P. This reduces the ion/atom ratio for Ca, producing a larger Ca(I) population in the plasma. Because of the lower temperature and n_e under the present operating conditions as compared to typical emission parameters, the ionization interferences were slightly worse in ICP-ICP-AFS compared to ICP-AES [13]. The enhancement of the Ca(I) signal was much larger than the depression of the Ca(II) fluorescence which was due to the higher population of Ca(II) and its relatively larger fluorescence sensitivity. The small depression in the large ion population caused by Na caused a large change in the relatively small atom population. This also illustrates the increased interelement effects which may be encountered if one were to choose a less sensitive emission or fluorescence line for analysis in order to increase the LDR or to avoid spectral interferences.

SRM Analysis

Several elements were determined in NBS SRM 364 (high carbon steel) with the atomization cell ICP operating at 1200 W. The weight percent solid concentrations ranged from 96.7% Fe to 0.0005% Zn. Only one sample solution (1.2206 g/L) was necessary to determine these elements by AFS (Cr, Cu, Zn) and RM (Fe), with the average relative error and relative standard deviation both being 1%. However, we did experience a problem with the analysis of Co. The measured concentration was 1.5 times the certified value. The same high value was measured at two different Co lines, which indicated that a spectral interference was probably not the cause. Zeeman AA yielded the correct result, which indicated that sample contamination did not cause the discrepency. This may have been due to a vaporization interference, but this had not been confirmed. No matrix matching of standards nor matrix blank was used. Only a solvent (acid) blank was employed. Even though the sample contained a large Fe concentration, no spectral interferences were encountered, despite the hundreds of Fe emission lines.

Conclusions

A log-log plot of S/N vs integration time displays a slope of 0.5, indicating that the present system is at the shot noise limit. Therefore, detection limits could be improved by increasing the signal integration time, but this improvement in LODs would only increase as the square root of the integration time. Further improvements in LODs may come about by using more efficient source collection optics, but this may be limited to a factor of two or three over the present system which employs f 1 optics. The major instrumental modification necessary

for this system to become a viable analytical instrument would be to combine the two r.f. generators and run the plasmas off a single 3 kW generator. The matching units would have to be slightly modified, but two 100 ohm units could be run in parallel off the single generator [50].

The versatility of ICP-ICP-AFS and RM is evident from its large LDR, up to 10^8, and LODs which are comparable to ICP-AES. The system should be considered an alternative to emission spectrometry in order to alleviate spectral interferences which may occur in complex sample matrices, without the need for an expensive, high resolution monochromator.

CHAPTER 5

FINAL COMMENTS AND SUMMARY

The effect of r.f. power on the shapes of the fluorescence curves has demonstrated that, in the extended sleeve torch, there are three groups of elements: the refractory, non-refractory, and alkaline earth elements. The behavior of the alkaline earth fluorescence signal vs power seems to indicate a complex relationship between the metal atom and the decomposition products of water. These elements form stable oxide, hydroxide, and dihydroxide molecules in flames and in plasmas which may account for this behavior. This work is inconclusive at this time because the measurements were all line of sight measurements, which do not afford the spatial resolution necessary to state conclusively the mechanism of this behavior. It has demonstrated, however, that care must be taken in the choice of an element which will be used to model the ICP, for example, calcium in many past studies. Also, the influence of water on the mechanism of the ICP must be considered, as was demonstrated by the dramatic effect water can have on the Ar(m) population.

The effect of propane on the atomization mechanism in the plasma has been investigated using fluorescence and emission spectrometry. The inert, monoatomic Ar atmosphere of the ICP has been shown to be an excellent atom and ion atomization cell for atomic fluorescence spectrometry because of its high atomization efficiency and quantum

efficiency. Propane, however, decreases the quantum efficiency of the plasma, although it does aid in the atomization of refractory elements and shifts the Saha equilibrium to produce a larger atom population by suppressing ionization in the ICP. Although this may enhance the fluorescence signal when only atomic transitions are considered, as in HCL-ICP-AFS, it does not improve the S/N of ICP-ICP-AFS [8].

The figures of merit for ICP-ICP-AFS are equal or superior to many atomic methods of analysis. The detection limits are comparable to ICP-AES for both the refractory and non-refractory elements, and the linear dynamic range is superior to all spectroscopic methods. This large LDR, up to eight orders of magnitude, is accomplished by combining the fluorescence and resonance monochromator curves of growth. The selectivity of the fluorescence technique when a narrow line source of excitation is used, as the ICP, results in very few spectral interferences. Even in the instances when these interferences occur, the interferent detection limit is usually three or more orders of magnitude higher than the LOD for the element of interest. This allows the use of a low resolution spectrometer for fluorescence detection without the need for background correction, as compared to ICP-AES which requires a high resolution monochromator and elaborate background correction schemes.

The use of the extended sleeve torch in fluorescence spectrometry also provides a long residence time for the sample in the hot plasma tail before it reaches the observation zone. This yields a high atomization efficiency and reduces the effect of solute vaporization interferences which can plague ICP-AES and flame spectrometry. By viewing the fluorescence signal at a height of 55 mm above the load coil, the

electronic temperature of the atomic vapor is relatively low producing a large free atom or ion ground state population to be probed while reducing the plasma background emission which can contribute to the background shot noise. However, because the plasma temperature is low, the electron number density is quite low which leads to a more pronounced ionization interference when large quantities of easily ionizable elements are present in the sample matrix.

The ICP-ICP-AFS system should be considered a viable alternative to ICP-AES when a large LDR is necessary and where spectral interferences must be minimized. However, this system is not expected to become commercially available because of several drawbacks, but could be assembled from existing laboratory equipment when the need for its special attributes is warranted. The drawbacks which limit the feasibility of this instrument are the need for two generators which may make the initial cost of such an instrument comparable to an ICP emission system with a high resolution polychromator. The operating costs are expected to be double that of an ICP-AES instrument because of the increase in power and argon consumption. Two minitorches, which are becoming popular in ICP-AES instruments, could be employed, thereby reducing the Ar consumption rate. Also, a single r.f. generator could be configured to run both plasmas. The instrument also has the drawback of being a sequential system, capable of analyzing only a single element at a time whereas several ICP emission systems permit simultaneous detection of up to fifty elements. The excitation solutions could be supplied to the excitation ICP by means of an auto-sampler, and the monochromator could be controlled so as to slew scan to each wavelength. This would automate the system to the point where it could be

competitive with sequential ICP-AES systems; however, the multi-element capabilities of ICP emission spectrometers with a direct reader could never be matched. Lastly, aspiration of a 2% excitation solution for long periods of time may become expensive, as in the case of the precious metals, and may be dangerous as in the case of many toxic metals such as Be, Hg, Pb, etc. The possible health hazard of aspirating concentrated solutions of toxic metals into the source ICP could be minimized or eliminated if a good hood/ventilation system was an integral part of the instrument. However, aspirating 2% solutions of the precious metals for extended lengths of time will be prohibitively expensive.

Nonetheless, employing an existing ICP emission system as an excitation source for exciting fluorescence in a second ICP may provide valuable information on a sample which could not be obtained by other atomic techniques.

ICP emission spectrometers have been slowly replacing atomic absorption spectrometers in the laboratory for routine analysis, and this trend seems likely to continue in the future. The main reasons for this are the larger linear dynamic range, excellent precision, reduced matrix effects, and multi-element capabilities of ICP-AES. Atomic fluorescence, on the other hand, possesses many of the attractive advantages of ICP-AES when an ICP is employed as an atomization cell; however, fluorescence systems are lacking in easy to use, high intensity excitation sources which may make them competitive with AES. The ideal AFS system of the future, in my opinion, will be a combination of ICP emission and fluorescence spectrometers. With a high resolution polychromator and the system operating in the emission mode, routine

multi-element analyses can be performed on a simultaneous basis. When spectral interferences occur which cannot be corrected by background correction techniques, the fluorescence mode can be employed. In this mode, a high intensity pulsed laser-dye laser combination can be employed to excite fluorescence of the atoms or ions of interest in the emission ICP. Because of the narrow bandwidth of the laser and the capability of doing non-resonance fluorescence, spectral interferences can be eliminated. Also, the fluorescence system can be employed when lower detection limits than AES must be achieved.

The complexity of present laser systems, and the high cost, at present make this system infeasible; however, the rapid developments in the field of electro-optics may produce a user friendly laser capable of satisfying the needs of an analytical instrument in the near future. I project that within 10 years, this type of ICP emission/fluorescence instrument will be commercially available to satisfy most analytical needs of the atomic spectroscopist. The knowledge we have gained by investigating atomic and ionic fluorescence in an ICP will play an integral part in development of this optimal atomic spectrometer.

APPENDIX A

GLOSSARY OF ACRONYMS AND ABBREVIATIONS

A	Einstein coefficient of spontaneous emission
AAS	atomic absorption spectrometry
AES	atomic emission spectrometry
AFS	atomic fluorescence spectrometry
B	Einstein coefficient of stimulated absorption (emission)
EDL	electrodeless discharge lamp
ETA	electro-thermal atomizer (graphite furnace)
FWHM	full width at half-maximum
HCL	hollow cathode lamp
ICP	inductively coupled plasma
ICP-ICP-AFS	ICP-excited ICP atomic/ionic fluorescence spectrometry
ICPMS	inductivity coupled plasma-mass spectrometry
k	collisional rate constant
LDR	linear dymanic range
LEAFS	laser-excited atomic fluorescence spectrometry
LEI	laser enhanced ionization
LOD	limit of detection
LTE	local thermodynamic equilibrium
NBS	national bureau of standards
PPB	parts per billion
PTE	partial thermodynamic equilibrium
RF	radio frequency radiation
RM	resonance monochromator
S/N	signal-to-noise ratio
SRM	standard reference material
Y	quantum efficiency

APPENDIX B

QUANTUM EFFICIENCY MEASUREMENTS

The quantum efficiency (Y) of a transition is the fraction of the absorbed energy which is converted into a fluorescence signal. The quantum efficiency is a guage of the quenching environment of an atom reservoir, and has a direct bearing on the intensity of the fluorescence signal. In analytical atomic fluorescence spectrometry, a high quantum efficiency atomization cell is desirable. A description of a simple 2-level system (Figure 19) is now presented and used to illustrate the significance and measurement of the quantum efficiency. Several excellent treatments of the intensity of transitions in spectrometry are available in the literature [30, 51-54], and the reader is referred to these for a more extensive description of these processes.

If an external light source impinges on an atom reservoir, two induced processes may occur. An atom in the ground state may absorb a photon with the probability per unit time of this stimulated absorption given by the Einstein probability of induced absorption (B_{12}) multiplied by the spectral energy density of the source (P_ν). The reverse process, stimulated emission, is governed by a similar expression, and has a rate of $B_{21}P_\nu$. Atoms in an excited state may emit a photon at an emission rate which is defined by the Einstein coefficient of spontaneous emission (A_{21}). These three processes are governed by the Einstein

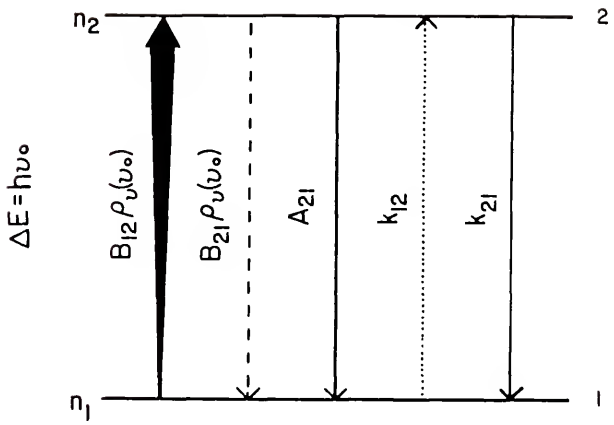

Figure 19. Schematic diagram of a 2-level atom. The ground state, level 1, has a population n_1 while the excited state, level 2, has a population n_2. The energy difference between the two levels, ΔE, is $h\nu_0$.

probability coefficients which are intrinsic properties of an atom, and do not depend on the atom's environment.

There are two other processes to be considered in the description of the 2-level system which are governed by the properties of the atom reservoir. Two collisional rate constants, k_{12} and k_{21}, define the nonradiative excitation and de-excitation processes which an atom may experience. In a given atom reservoir, an atom may be excited by a collision with another specie at a rate of k_{12}. Analogously, an atom in an excited state may decay to the ground state upon collision with another specie without the emission of a photon. This radiationless deactivation rate is expressed as k_{21}.

Because of the low source spectral irradiance of the laser employed in this study, the rate of stimulated emission ($B_{21}P_{\nu}$) can be neglected, because a linear interaction between the source radiation and the atomic system is maintained. In other words, $B_{21}P_{\nu}$ is negligible if saturation is not approached.

Lifetime measurements of a 2-level atom can be used to determine the quantum efficiency. The spontaneous radiative lifetime of a transition is defined as

$$\tau_{sp} = \frac{1}{A_{21}} ,$$

while a purely nonradiative lifetime can analogously be defined as

$$\tau_{nr} = \frac{1}{k_{21}} .$$

The fundamental parameter that defines the influence of collisions which depopulate the excited state, namely the quantum efficiency of the transition (Y_{21}), can be described by combining the above two expressions. The quantum efficiency is the probability that the excited atom will lose its energy by the emission of a photon, and is defined as

$$Y_{21} = \frac{A_{21}}{A_{21} + k_{21}}$$

in terms of the rate coefficients, or in terms of the lifetime of the excited state,

$$Y_{21} = \frac{\tau_{obs}}{\tau_{sp}}$$

where τ_{obs} is the observed or measured lifetime of the transition. Therefore, by measuring the excited state lifetime and knowing the spontaneous lifetime (or A_{21}), a value for the quantum efficiency of the transition can be obtained. Reports of lifetime measurements in the literature are very scarce because most atomic τ_{sp} are on the order of a few ns. Also, many atoms reservoirs, such as flames, have very low quantum efficiencies which shortens the observed lifetimes to values below 1 ns, which are very difficult to measure.

When a temporally narrow excitation light source impinges upon an atom reservoir containing Na atoms at time t = 0, the fluorescence decay curve depicted in Figure 20 is produced. As can be seen, simply by measuring the time it takes for the fluorescence intensity to decay by

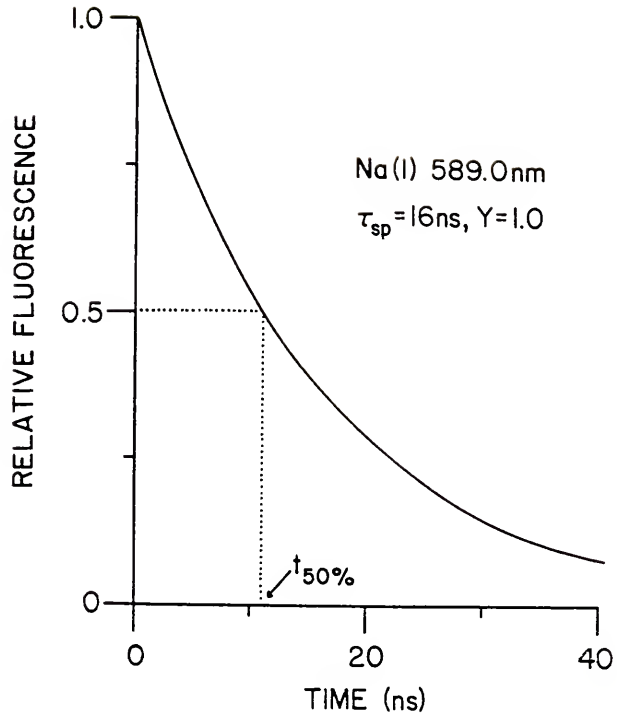

Figure 20. Fluorescence decay curve for Na.

50% (or some other convenient value), one can determine the radiative lifetime from the exponential decay expression

$$F(t) = F_{max} e^{-t/\tau_{obs}} ,$$

where F(t) is the fluorescence signal at time t, F_{max} is the maximum fluorescence signal, and τ is the observed lifetime of the transition. From the measurement of the time it takes for the fluorescence signal to decay to 50% of its maximum value ($t = t_{50\%}$, $\frac{F(t)}{F_{max}} = 0.5$), the above equation reduces to

$$\tau_{obs} = \frac{t_{50\%}}{0.693} .$$

This was the procedure used in this study to determine the quantum efficiencies of Na and Li in the ICP. A high value for Y demonstrates that the atom reservoir is an excellent choice for atomic fluorescence measurements, as long as the atomization efficiency is also high. For the ICP, both the quantum efficiency and atomization efficiency are very high, making it an attractive atomization cell and atom reservoir for AFS.

APPENDIX C

COMPARATIVE DETECTION LIMITS

The ultimate goal of analytical atomic spectrometry is to be able to detect single atoms. Single atom detection has been achieved in certain special cases, and schemes have been proposed to determine single atoms by a variety of methods [55-56]. However, most analytical methods possess detection limits in the parts per billion or parts per trillion range, clearly, many order of magnitude above single atom detection. But what is the significance of these detection limits? Surely if one technique possesses lower LODs, it would be the method of choice for a particular analysis. Unfortunately, this is the view of many analytical chemists, and can lead to tragedy if all the figures of merit for a particular technique are not viewed together.

In 1978, the International Union of Pure and Applied Chemists (IUPAC) adopted a model for the calculations of LODs [57], a model which was also approved by the American Chemical Society (ACS) Subcommittee on Environmental Analytical Chemistry in 1980 [58]. Even though a standard method for determining LODs has been presented, many spectroscopists, and chemists in general, refuse to employ this method and continue to calculate LODs by their own methods. This can lead to a great diversity in detection limits reported for the same method, which leads to LODs that can easily vary by an order of magnitude or more through the use of

different statistical methods [59]. For the purpose of this work, the IUPAC definition was used to calculate the LODs. This definition is:

$$LOD = \frac{kS_b}{m} ,$$

where k is a scale factor which determines the confidence level, S_b is the standard deviation of the blank readings, and m is the slope of the calibration curve, often referred to as the sensitivity. Typically, a k value of 2 or 3 is chosen in the calculation of the LOD: however, k values vary depending on the researcher. The standard deviation of the blank, S_b, also depends upon the method used to calculate and measure this quantity. Because the standard deviation is only valid for an infinitely large number of measurements, S_b is only an approximation of the actual standard deviation and depends on the number of blank reading used to calculate this parameter. When reported in the literature, most standard deviations are calculated from 10 to 25 measurements, although reports of standard deviations for only two measurements have made their way into publication.

It is clearly evident that there exists a diversity of methods used to determine LODs [59], and extreme care must be taken when comparing detection limits from different sources. LODs should only be used as approximations of the minimum concentration which can be detected under the optimum conditions (detection limits are typically determined under the optimal experimental conditions using the simplest matrix available, usually, high purity salts dissolved in the purest water available). Actual quantitative determinations usually require an analyte

concentration between 5 and 10 times the calculated LOD, while some samples with complex matrices require the analyte to be present at 50 to 100 times the LOD before meaningful results can be obtained.

Bearing all these factors in mind, Table 7 presents a comparison of typical detection limits and linear dynamic ranges for several atomic spectrometric methods. A more complete comparison of LODs and the historical progression of detection limits over the past two decades is given in reference 60.

At this point, a few comments on Table 7 are necessary to put the tabulated values in perspective. Methods employing electrothermal atomizers, commonly referred to as graphite furnaces, possess some of the best detection limits obtained. However, furnaces suffer from many vaporization interferences which usually require the use of matrix modifiers to reduce these effects [14]. In many cases, a different matrix modifier is required for each element, or group of elements, which is to be determined in a complex sample matrix. This tends to make sample preparation and methods development very time consuming, and does not insure the elimination of matrix effects.

Methods which employ lasers as excitation sources, AFS and laser enhanced ionization (LEI), also exhibit very low LODs. However, lasers are notoriously noisy, having shot-to-shot instabilities ranging from a few percent up to 20%. These instabilities, or pulse-to-pulse shot noise, can be eliminated if the laser has enough power to saturate the transition being studied [52]; however, most laser systems available today cannot optically saturate transitions below approximately 300 nm. This is a significant drawback, since most of the intense atomic resonance transitions lie between 180-300 nm. Another significant

Table 7. Comparison of Atomic Spectrometric Methods.

METHOD	SOURCE	CELL	LOD(ppb)[a]	LDR(decades)[b]
AFS	Laser	Flame	1-1,000	3-6
		ETA	0.001-1,000	2-5
		ICP	0.1-1,000	3-6
	HCL	ICP	0.1-1,000	3-5
	Xe Arc	Flame	1-1,000	2-4
	ICP	ICP	0.1-100	4-8
		Flame	1-1,000	4-7
LEI	Laser	Flame	0.001-100	3-6
AAS	HCL	Flame	1-1,000	1-3
		ETA	0.001-100	1-3
AES		ICP	0.1-100	2-5
		Flame	0.1-10,000	2-5
ICP-MS		ICP	0.01-10	2-4

[a]Range of LODs, in parts per billion, commonly found in the literature.

[b]Linear working range of the calibration curve in decades (orders of magnitude).

drawback to employing laser systems is that they are expensive, in the initial cost of the system and in the maintenance costs. These systems have also not become "user friendly," as have many computer systems over the past few years, making them difficult to operate on a daily basis. Because of their complexity, it is often necessary to spend several hours to tune a laser to a particular atomic transition, making them ineffective as multi-element sources.

Inductively coupled plasma-mass spectrometry (ICP-MS) is the most recently introduced technique listed in Table 7. On the surface, this technique has excellent detection limits and has the unique capability of being able to determine isotope ratios of the elements contained in the sample [61-62]. However, ICP-MS is plagued with spectral interferences and many matrix effects. The spectral interferences arise from the many isotopes of both atomic and molecular species which are present in the ICP. For many elements, especially the refractory elements, a large percentage of the total element is in the form of molecular species, typically oxides and hydroxides. If these molecular peaks coincide with the analyte element's peak, a spectral interference, not unlike spectral interferences in ICP-AES, will occur. Also, many matrix effects exist in ICP-MS. Although the instruments manufacturers refer to these matrix effects as "apparent matrix effect," they are very real, and may eventually cause this technique to be abandoned within the next few years if these problems are not resolved [64].

In summary, LODs are useful in comparing one spectroscopic technique to another, if the same method is used for their determination. Beyond only a superficial comparison, though, LODs should be used in conjunction with all the figures of merit for a given method of

analysis. Linear dynamic range, spectral and matrix interferences, ease of operation of the instrument, sample preparation requirements, and instrument cost should all be incorporated into the evaluation of a particular technique. Also, many applications do not require detection limits in the parts per trillion range. In these instances, a particular technique should be chosen on the basis of whether or not it can satisfy the analysis requirements, and not on the basis of which technique possesses the best LODs. In short, LODs are a guide to analytical performance, and not the only figure of merit which describes the utility of the technique or method.

REFERENCES

[1] T.B. Reed, J. Appl. Phys. 32, 821 (1961).

[2] S. Greenfield, I.L. Jones, and C.T. Berry, Analyst 89, 713 (1964).

[3] R.H. Wendt and V.A. Fassel, Anal. Chem. 37, 920 (1965).

[4] N. Omenetto, S. Nikdel, J.D. Bradshaw, M.S. Epstein, R.D. Reeves, and J.D. Winefordner, Anal. Chem. 51, 1521 (1979).

[5] M.S. Epstein, N. Omenetto, S. Nikdel, J. Bradshaw, and J.D. Winefordner, Anal. Chem. 52, 284 (1980).

[6] N. Omenetto, P. Cavalli, and G. Rossi, Rev. Anal. Chem. 5, 185 (1982).

[7] M.A. Kosinski, H. Uchida, and J.D. Winefordner, Anal. Chem. 55, 688 (1983).

[8] G. L. Long and J.D. Winefordner, Appl. Spectrosc. 38, 563 (1984).

[9] R.J. Krupa, G.L. Long, and J.D. Winefordner, Spectrochim. Acta 40B, 1485 (1985).

[10] H.G.C. Human and R.H. Scott, Spectrochim. Acta 31B, 459 (1976).

[11] R.K. Winge, V.J. Peterson, and V.A. Fassel, Appl. Spectrosc. 33, 206 (1979).

[12] D.R. Demers, Spectrochim. Acta 40B, 93 (1985).

[13] G.F. Larson and V.A. Fassel, Anal. Chem. 48, 1161 (1976).

[14] G.F. Kirkbright and M. Sargent, Atomic Absorption and Fluorescence Spectroscopy, Academic Press, London (1974).

[15] J.W. Carr, M.W. Baldes, and G.M. Hieftje, Appl. Spectrosc. 36, 689 (1982)

[16] S.R. Koirtyohann, Personal communication, University of Missouri (1984).

[17] C.A. Monnig and S.R. Koirtyahann, Appl. Spectrsc. 39, 884 (1985).

[18] L.M. Fraser and J.D. Winefordner, Anal. Chem. 44, 1444 (1972).

[19] D.R. Demers and C.D. Allemand, Anal. Chem. 53, 1915 (1981).

[20] J.J. Leary, A.E. Brooks, A.F. Dorrzapf, Jr., and D.W. Golightly, Appl. Spectrosc. 36, 37 (1982).

[21] M.W. Routh, P.A. Wartz, and M.B. Denton, Anal. Chem. 49, 1422 (1977).

[22] L.R. Porker, Jr., N.H. Tioh, and R.M. Barnes, Appl. Spectroc. 39, 45 (1985).

[23] S. Greenfield, P.B. Smith, A.E. Breeze, and N.M.D. Chilton, Anal. Chim. Acta 41, 385 (1968).

[24] B. Magyar and F. Aeschbach, Spectrochim. Acta 35B, 839 (1980).

[25] R.H. Wendt and V.A. Fassel, Anal. Chem. 38, 337 (1966).

[26] J.D. Windfordner and T.J. Vickers, Anal. Chem. 36, 1947 (1964).

[27] M.L. Parsons, B.W. Smith, and G.E. Bentley, Handbook of Flame Spectroscopy, Plenum Press, New York (1975).

[28] R. Mavrodineanu and H. Boiteux, Flame Spectroscopy, John Wiley and Sons, Inc., New York (1965).

[29] C.H. Corliss and W.R. Bozman, Experimental Transition Probabilities for Spectral Lines of Seventy Elements, NBS Monograph 53, Washington, DC (1962).

[30] C. Th. J. Alkemade, T. Hollander, W. Snellman, and P.J.Th. Zeegers, Metal Vapours in Flames, Pergamon Press, New York (1982).

[31] R.N. Savage and G.M. Hieftje, Anal. Chem. 52, 1267 (1980).

[32] M.A. Kosinski, H. Ulchida, and J.D. Winefordner, Talanta 30, 339 (1983).

[33] M.W. Blades and G. Horlick, Spectrochim. Acta 36B, 881 (1981).

[34] P.J.Th. Zeegers, W.P. Townsend, and J.D. Winefordner, Spectrochim Acta 24B, 243 (1969).

[35] H. Uchida, M.A. Kosinski, N. Omenetto, and J.D. Winefordner, Spectrochim. Acta 38B, 529 (1983).

[36] S. Huang, D. Mo, K.S. Yeah, and J.D. Winefordner, in press, Canad. J. Spectrosc. (1986).

[37] R.S. Houk, V.A. Fassel, and B.R. LaFreniere, Appl. Spectrosc. 40, 94 (1986).

[38] D.R. Jenkins, Spectrochim. Acta 25B, 47 (1970).

[39] G.F. Kirkbright, Chapter in Developments in Atomic Plasma Specrochemical Analysis, R.M. Barnes (ed), Heyden Press, London (1981).

[40] W.H. Gunter, K. Visser, and P.B. Zeeman, Spectrochim. Acta 37B, 571 (1982).

[41] Plasma/AFS Comparative Detection Limits, Baird Corporation, Bedford, MA (1985).

[42] Plasma/AFS Precious Metal Analysis Bulletin, Baird Corporation, Bedford, MA (1985).

[43] Periodic Table of Detection Limits and Upper Linear Range for ICP-AES, Allied Analytical Systems, Andover, MA (1985).

[44] P.J.T. Zeegers, R. Smith, and J.D. Winefordner, Anal. Chem. 40, 26A (1968).

[45] D. Demers, Personal communication, Baird Corporation, Bedford, MA (1985).

[46] G.F. Larson and V.A. Fassel, Appl. Spectrosc. 33, 592 (1979).

[47] P.W.J.M. Boumans, Line Coincidence Tables for Inductively Coupled Plasma Atomic Emission Spectrometry, Vols. 1 and 2, Pergamon Press, New York (1980).

[48] G.R. Harrison, Massachusetts Institute of Technology Wavelength Tables, M.I.T. Press, Cambridge, MA (1969).

[49] B.L. Coughlin and M.W. Blades, Spectrochim. Acta 39B, 1583 (1984).

[50] S. Barber, Personal communication, R.F. Plasma Products, Inc., Cherry Hill, N.J. (1985).

[51] A.P. Thorne, Spectrophysics, Science Paperbacks, London (1974).

[52] N. Omenetto (ed), Analytical Laser Spectrometry, John Wiley, New York, (1979).

[53] A.C.G. Mitchell and M.W. Zemansky, Resonance Radiation and Excited Atoms, University Press, Cambridge, England (1961).

[54] N. Omenetto and J.D. Winefordner, Prog. Analyt. Atom. Spectrosc. 2, 1 (1979).

[55] G.S. Hurst, M.G. Payne, S.D. Kramer, and C.H. Chen, Phys. Today 33, 24 (1980).

[56] C. Th. J. Alkemade, Appl. Spectrosc. 35, 1 (1981).

[57] International Union of Pure and Applied Chemists, Spectrochim. Acta 33B, 242 (1978).

[58] American Chemical Society, Anal. Chem. 52, 2242 (1980).

[59] G.L. Long and J.D. Winefordner, Anal. Chem. 55, 712A (1983).

[60] M.L. Parons, S. Major, and A.R. Forster, Appl. Spectrosc. 37, 411 (1983).

[61] V. Fassel, paper no. 1, Pittsburgh Conference on Analytical Chemistry and Applied Spectroscopy (1986).

[62] R.S. Houk, paper no. 2, Pittsburgh Conference on Analytical Chemistry and Applied Spectroscopy (1986).

[63] R.C. Hutton, J.E. Cantle, and D.E. Kelly, paper no. 229, Pittsburgh Conference on Analytical Chemistry and Applied Spectroscopy (1986).

[64] G. Horlick, S.H. Tan, M.A. Vaughn, Y. Shao, and J. Lam, paper no. 226, Pittsburgh Conference on Analytical Chemistry and Applied Spectroscopy (1986).

BIOGRAPHICAL SKETCH

Robert Joseph Krupa was born in Holyoke, Massachusetts, on July 12, 1960. He attended Georgetown Preparatory School in Rockville, Maryland, and graduated from Marquette University in Milwaukee, Wisconsin, with a B.S. in chemistry in 1982. Since that time he has attended the University of Florida where he received his Ph.D. in chemistry in 1986 under the direction of Dr. James D. Winefordner.

I certify that I have read this study and that in my opinion it conforms to acceptable standards of scholarly presentation and is fully adequate, in scope and quality, as a dissertation for the degree of Doctor of Philosophy.

James D. Winefordner
Graduate Research Professor of Chemistry

I certify that I have read this study and that in my opinion it conforms to acceptable standards of scholarly presentation and is fully adequate, in scope and quality, as a dissertation for the degree of Doctor of Philosophy.

John G. Dorsey
Associate Professor of Chemistry

I certify that I have read this study and that in my opinion it conforms to acceptable standards of scholarly presentation and is fully adequate, in scope and quality, as a dissertation for the degree of Doctor of Philosophy.

Eric R. Allen
Professor of Environmental Engineering

This dissertation was submitted to the Graduate Faculty of the Department of Chemistry in the College of Liberal Arts and Sciences and to the Graduate School and was accepted as partial fulfillment of the requirements for the degree of Doctor of Philosophy.

August, 1986

Dean, Graduate School